



Title: Response of Flexible Risers in Bend Stiffener Area	Delivered: 15.06.2011
	Availability: OPEN
Student: Kim Løseth	Number of pages: 66 + Appendix

Abstract:

Flexible risers is a vital part of a floating production system (FPS). In order to predict the riser life time, many procedure may be applied.

In this thesis it is assumed that the pipe could be represented with help of performing two sets of global anlaysis. Where in the first set it is assumed that the bending stiffness of the pipe is similar to the stick region of the flexible pipe and in the second part the bending stiffness it is assumed a bending stiffness similar to the slip regime of the flexible pipe. The dynamic analysis for these two sets is performed in SIMLA, which is mainly a special purpose tool for pipe laying, but robust enough for to perform most of pipeline engineering problems. The analysis is set to be from a semi submersible in typical North Sea loading conditions. The nodal displacement time series obtained from these analysis is then stored into blocks with constant amplitude loading for the upper part of the riser configuration.

The results obtained from the global analysis is then used as inputs for a local analysis performed in BFLEX2010, which is a special purpose FEM software for stress analysis of flexible pipes. The local analysis is mostly focused on the fatigue of the flexible riser and it is performed an investigation from the effect of introducing different gaps between the pipe and the bend stiffener. The data obtained from these analysis, results in more distributed stress concentration within the bends stiffener region, especially for the largest sea states. There is also performed analysis where it is assumed no contact interference with the bend stiffener and the pipe, where it results in a much larger stress concentration at the hang of region, and a more even stress distribution along the riser.

Keyword:

Flexible risers
BFLEX2010
SIMLA

Advisor:

Prof. Svein Sævik - NTNU



THESIS WORK SPRING 2011

for

Stud. tech. Kim Løseth

Response of Flexible Risers in the Bend Stiffener Area

Respons av fleksible stigerør i bøyestiverområdet

The flexible riser is a vital part of a floating production system. In order to predict the riser lifetime for given environmental conditions, different analysis procedures may be applied, however, in most cases including the three fundamental steps:

1. Global dynamic analysis of the riser system in order to find the global response quantities in the form of time series of tension and curvature. This is obtained by a global analysis software such as the Marintek softwares RIFLEX and SIMLA.
2. Transform the global response quantities into into time series of stresses using a local analysis tool such as the Marintek software BFLEX.
3. Group the time series of stress into classes of stress ranges and combine these with fatigue S-N data to obtain the Miner sum, i.e. the accumulated fatigue damage throughout the lifetime of the riser.

When it comes to the global dynamic analysis different assumptions have traditionally been applied with regard to the bending stiffness of the riser:

1. Assume that the layers are in the sliding regime and estimate the bending stiffness as the sum of contributions from the plastic layers.
2. Assume that the layers are in the stick regime, the bending stiffness being similar to a steel pipe of same dimension.
3. Use a model that is based on the true moment-curvature behaviour.

This thesis work focus on investigating the effect of applying different modelling assumptions with respect to the fatigue damage in the bend stiffener (BS) area of the flexible risers. The thesis work will be based on the models established in the project work and is to be carried out as follows:

1. Literature study, including flexible pipe technology, failure modes and design criteria, methods and techniques for global and local analysis of flexible risers.
2. Familiarize with the Marintek softwares SIMLA and BFLEX.
3. Establish two models in SIMLA for global analysis of a flexible riser using a relative coarse element meshing of the BS section, one based on the sliding plastic EI and the other based on the stick EI (items 1 and 2 above).
4. Divide the scatter diagram into a relevant number of blocks and perform non-linear irregular sea simulations of 1 hour duration for each block and for each model. Use the y-rotation as master time series and perform rainflow counting of

- the top tension and the y-rotation. Use that to obtain classes of max and min angles as well as associated mean tensions for each class. For how many classes is the friction moment exceeded in the stick model?
5. Establish one detailed model in BFLEX2010 for the BS section and use the developed classes to perform fatigue calculation of the tensile armour layers. The BFLEX model is to be based on contact elements between the pipe and the BS assuming a certain gap. Vary the gap and investigate its influence on the fatigue damage.
 6. Conclusions and recommendations for further work

The work scope may prove to be larger than initially anticipated. Subject to approval from the supervisors, topics may be deleted from the list above or reduced in extent.

In the thesis the candidate shall present his personal contribution to the resolution of problems within the scope of the thesis work

Theories and conclusions should be based on mathematical derivations and/or logic reasoning identifying the various steps in the deduction.

The candidate should utilise the existing possibilities for obtaining relevant literature.

Thesis format

The thesis should be organised in a rational manner to give a clear exposition of results, assessments, and conclusions. The text should be brief and to the point, with a clear language. Telegraphic language should be avoided.

The thesis shall contain the following elements: A text defining the scope, preface, list of contents, summary, main body of thesis, conclusions with recommendations for further work, list of symbols and acronyms, references and (optional) appendices. All figures, tables and equations shall be numerated.

The supervisors may require that the candidate, in an early stage of the work, presents a written plan for the completion of the work.

The original contribution of the candidate and material taken from other sources shall be clearly defined. Work from other sources shall be properly referenced using an acknowledged referencing system.

The report shall be submitted in two copies:

- Signed by the candidate
- The text defining the scope included
- In bound volume(s)
- Drawings and/or computer prints which cannot be bound should be organised in a separate folder.

Ownership

NTNU has according to the present rules the ownership of the thesis. Any use of the thesis has to be approved by NTNU (or external partner when this applies). The department has the right to use the

thesis as if the work was carried out by a NTNU employee, if nothing else has been agreed in advance.

Thesis supervisors

Prof. Svein Sævik, NTNU.

Dr. Gro Sagli Baarholm, Marintek.

Deadline: June 14th, 2011

Trondheim, January 19th, 2011

Svein Sævik

Candidate - signature and date:



Preface

This report is the result of the M.Sc. thesis which is the part of the two year master program in Underwater Technology at the Norwegian University of Science and Technology (NTNU). This thesis is written in the last semester under the course name *TMR4900 Marine Structure* and weighted 30 units.

This thesis consist of a literature study and an anylsis part, and are in a some way building upon the project thesis, from the course TMR4505, with the following title *Hysteresis damping of flexible risers*. However, this is pretty much a stand alone report, with not much connection to the project thesis.

The literature study part is performed to provide a good knowledge about flexible riser systems, give a good introduction to the computer software used in this thesis, BFLEX2010 and SIMLA and and knowledge about typical solution techniques obtained in such numerical software.

In analysis part it is performed with a basis of knowledge obtained in the literature study.

As the work progressed I have met on several challenges, most of them regarding performing sufficient analysis in an efficient way. Many anylsis had to be performed several times, resulting in a high amount of compiling time. However, by with help of Linux based script to run several analysis in series, without any human interaction between them, this part was done in a acceptable amount of time.

It is assumed here that persons reading this report has some background knowledge of the thermology and theory presented in this report.

I would like to thank Professor Svein Sævik for guideence with this thesis.

Trondheim, June 14, 2011

Kim Løseth



Abstract

Flexible risers is a vital part of a floating production system (FPS). In order to predict the riser life time, many procedure may be applied.

In this thesis it is assumed that the pipe could be represented with help of performing two sets of global analysis. Where in the first set it is assumed that the bending stiffness of the pipe is similar to the stick region of the flexible pipe and in the second part the bending stiffness it is assumed a bending stiffness similar to the slip regime of the flexible pipe. The dynamic analysis for these two sets is performed in SIMLA, which is mainly a special purpose tool for pipe laying, but robust enough for to perform most of pipeline engineering problems. The analysis is set to be from a semi submersible in typical North Sea loading conditions. The nodal displacement time series obtained from these analysis is then stored into blocks with constant amplitude loading for the upper part of the riser configuration.

The results obtained from the global analysis is then used as inputs for a local analysis performed in BFLEX2010, which is a special purpose FEM software for stress analysis of flexible pipes. The local analysis is mostly focused on the fatigue of the flexible riser and it is performed an investigation from the effect of introducing different gaps between the pipe and the bend stiffener. The data obtained from these analysis, results in more distributed stress concentration within the bends stiffener region, especially for the largest sea states. There is also performed analysis where it is assumed no contact interference with the bend stiffener and the pipe, where it results in a much larger stress concentration at the hang of region, and a more even stress distribution along the riser.



Contents

Preface	i
Abstract	ii
List of Figures	v
List of Tables	vii
1 Introduction	1
1.1 Flexible pipe cross section	2
1.1.1 Carcass	3
1.1.2 Pressure armour	4
1.1.3 Tensile armour	4
1.2 Inner and outer liner	5
1.2.1 Additional layers	5
1.3 Riser configurations	5
1.4 Termination of riser	8
1.5 Design requirements	9
2 Mechanical description	10
2.1 Axis-Symmetrical loads	10
2.2 Bending loads	11
3 Fatigue analysis	14
3.1 The SN-approach	14
3.2 Cycle counting	15
3.2.1 Peak counting	16
3.2.2 Rainflow counting	16
3.3 Accumulated damage	18
3.4 Fatigue analysis for flexible risers	19
4 Software theory	20
4.1 SIMLA	20
4.1.1 System structure	20
4.1.2 Principle of virtual displacement	21
4.1.3 Static analysis	22
4.1.4 Dynamic analysis	22
4.1.5 Pipe element definition	24
4.1.6 Material models	24
4.1.7 Hydrodynamic loading	25



4.1.8	Wave kinematics	26
4.2	BFLEX2010	28
4.2.1	Similarity to SIMLA	29
4.2.2	Bending formulation	29
5	Global analysis	31
5.1	Model description	31
5.1.1	Modeling of riser configuration	31
5.1.2	Environmental data	33
5.1.3	Simulation	34
5.1.4	Results of interest	35
5.2	Results	36
5.2.1	Static results	36
5.2.2	Stick regime	38
5.2.3	Slip regime	40
5.2.4	Conclusion	42
6	Local analysis	43
6.1	Model description	43
6.1.1	Bending stiffener	45
6.1.2	Lifetime data	46
6.1.3	Simulation	47
6.2	Results	48
6.2.1	Part 1	48
6.2.2	Part 2	51
7	Conclusion	54
8	Suggestion to further work	55
A	Flexible riser data	A
B	Cross Sectional Properties	B



List of Figures

1	Floating production System	1
2	Cross section of an unbonded pipe[18]	3
3	Carcass profile [1]	4
4	Zeta profile [1]	4
5	Riser configurations [2]	7
6	Schematic illustration of a bending stiffener [2]	8
7	Response models for cross-sectional analysis [12]	10
8	Flexible pipe subjected to axial force	11
9	Bending behavior of flexible pipe	12
10	Definition of thendon position (θ)	13
11	SN-curves in sea water with cathodic protection [17].	15
12	Peak counting of a narrow banded load history	16
13	Rainflow counting of an broad banded load history	17
14	Illustration of typical two different offshore load spectra	18
15	SIMLA system architecture	21
16	Newton-Raphson iteration	23
17	Pipe element in SIMLA	25
18	BFLEX2010 System structure [15]	29
19	Dimensions of riser configuration	31
20	Bending - Curvature relationship $p_{int}=475$ bar	32
21	Results of interest	35
22	Dynplot series of nodal displacement in pitch	36
23	Static axial tension distribution along the riser length coordinates	37
24	Enveloped curvature of riser in stick regime (Sea state 18)	38
25	Dynplot series of nodal rotation about the local y-axis	39
26	Load counting in stick regime	39
27	Enveloped curvature of riser in slip regime	40
28	Dynplot series of nodal rotation about the local y-axis	41
29	Smoothed response in slip regime	41
30	Load counting in slip regime	42
31	Local BFLEX2010 model (Not in scale)	43
32	Mesh of BFLEX2010 model	44
33	θ -series constraint	45
34	Bending stiffener design	45
35	Maximum stress location - Block 14 - Slip regime- Part 1	48
36	Fatigue distribution - Slip regime - Part 1	48
37	Block damage from stick regime	49
38	Block damage from slip regime	50



39	Stress distribution in tensile armour $t = 180$	51
40	Fatigue damage from part 2	51
41	Curvature distribution for block 10 in slip regime, $t = 100$. . .	53
42	Curvature distribution for block 4 in slip regime, $t = 100$. . .	53



List of Tables

1	Unbonded pipe families [1]	2
2	Flexible pipe design criteria [1]	9
3	Results from peak counting	16
4	Results from rainflow counting	17
5	Pipe properties	32
6	Blocked scatter diagram, Statfjord field [7]	33
7	Simulation of cases	34
8	Pipe properties	43
9	Gap cases	46
10	SN-curve data	46
11	Simulation of BFLEX2010 cases	47
12	Part 1 results	49
13	Part 2 results	52



1 Introduction

The flexible riser is a vital part of floating production systems (FPS) all over the world, picture 1. Compared to ordinary rigid carbon steel risers, it has an ability to work under extreme dynamic conditions. And it is therefore recommended in many cases.

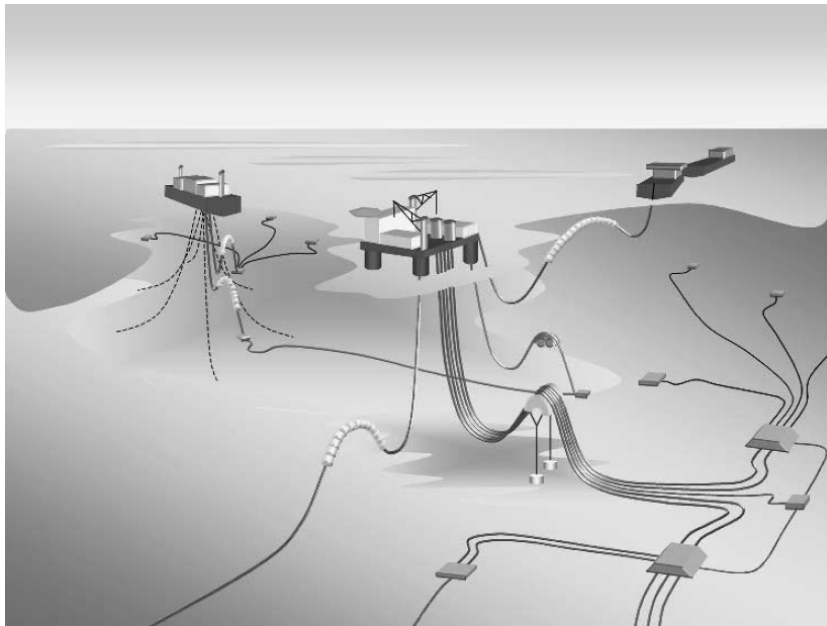


Figure 1: Floating production System

Flexible pipes used in a riser configuration has an wide range of functions, mainly [4];

- Well product flow (oil, gas, condensate)
- Well control lines, annulus flow, electric , hydraulic, optical, etc.
- Injection lines for water and gas.
- Processed product export.

The flexible pipe has been used since the late 70's [3], and from there, especially since the early 90's, the use of flexible pipes in more and more extreme conditions has been rapidly increased. There is now used flexible pipes in depths up to 8000 feet, and pipes with internal pressure up to 15000 psi, and temperatures up to 130°C [3]. However, this progress has not been without failures, numbers from Statoil says that there has been



performed 8 recently/ongoing replacement project of flexible risers [10]. With this in mind, and a still desire for greater depths and higher pressures, there has been performed new guidelines to ensure better integrity on flexible risers [9].

1.1 Flexible pipe cross section

Flexible pipes basically consist of two types of components; armouring and sealing components. In combination of these two components there is typically designed two different types of flexible pipes;

- **Bonded**, consist of monolithic armour and sealing components, where the deformation of the sealing components is relative to the motion of neighboring armour components.
- **Unbonded**, consist of cylindrical layers, where the armour layers are allowed to slide relative to the neighboring sealing layers.

Bonded flexible pipe is mostly used when short lengths are needed, due to an limitation of length per segment, typical under 100 meters for 4-10” pipes. Therefore typical applications for bonded flexible pipes are jumper lines, loading hoses and kill/choke lines. For long lengths, pipe joints are required. In other words, bonded flexible pipe is not often used in riser configurations. Unlike the bonded pipe, can the unbonded pipe be constructed in lengths up to several kilometers. And in this way make the unbonded pipe preferred in riser configurations.

It’s normal to divide unbonded flexible pipe into 3 product families, a requirement for these 3 different families is described in table 1.

Table 1: Unbonded pipe families [1]

Layer No.	Layer primary function	Product family I Smooth-bore pipe	Product family II Rough-bore pipe	Product family III Rough-bore, reinforced pipe
1	Prevent collapse	Pressure-armour layer(s)	Carcass	Carcass
2	Internal fluid integrity	Internal pressure sheath	Internal pressure sheath	Internal pressure sheath
3	Hoop stress resistance	Pressure-armour layer(s)	—	Pressure-armour layer(s)
4	External fluid integrity	Intermediate sheath	—	—
5	Tensile-stress resistance	Crosswound tensile armours	Crosswound tensile armours	Crosswound tensile armours
6	External fluid integrity	Outer sheath	Outer sheath	Outer sheath

Table 1 is only covering the minimum requirement for the 3 families, and it's not unusual to make flexible pipes with up to 20 layers. A typical cross section of an unbonded flexible pipe, product family III, is illustrated in figure 2 and discussed in the following subsections.

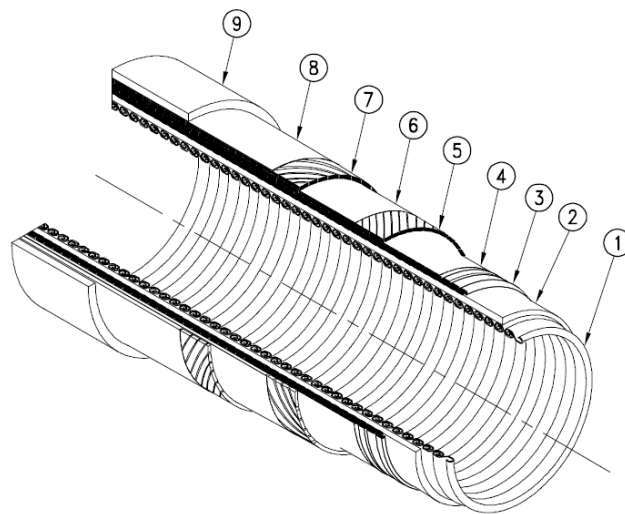


Figure 2: Cross section of an unbonded pipe[18]

1.1.1 Carcass

Layer 1 is the carcass and it is the innermost layer of the pipe. It consist of an open interlocking profile, figure 3, layed with an high lay angle relative to the longitudinal pipe axis. Since this layer is in direct contact with the bore fluid the material depends on the fluid chareceristics, mostly regarding corrosion problem. The function of the carcass is to provide strength due to hydrostatic external pressure, as well as crushing loads under installation. The most common materials used is the AISI grades 304 and 316, and Duplex steel [3].

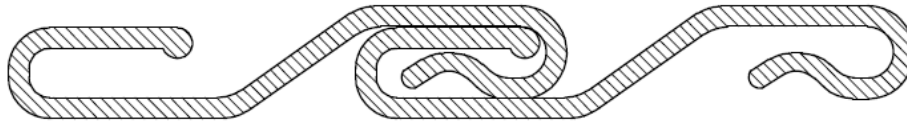


Figure 3: Carcass profile [1]

1.1.2 Pressure armour

Layer 3 in figure 2 is the pressure armour layer. This layer consist of an interlocking profile, typical like the zeta profile in figure 4, but other designs are known in use. Like the carcass, this layer is also layed with a high lay angle. The main application for the pressure armour is to substain loads due to internal pressure, but also supporting the carcass against high external pressure and accidental loads. The pressure armour is typical made of low-alloyed carbon steel grades, with a typical high yield strength, in the range of 800-1000MPa.

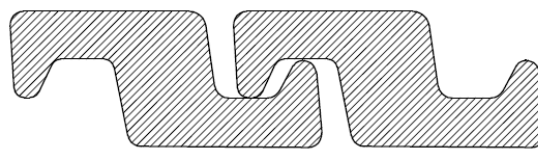


Figure 4: Zeta profile [1]

1.1.3 Tensile armour

Layer 7 and 6 in figure 2 is a pair of tensile armour. The tensile armour consist of typical two or four cross wounded layers, made of flat rectangular wires layed in a low angle relative to the longitudinal pipe axis (typical 30°-50°). The tensile armour is providing strength in longitudinal direction and gives support to the weight of all the layers and transerfing it to end



termination point on the vessel/structure. The tensile armour is also transferring some of the longitudinal load into an inward radial force analogous to the external pressure. The tensile armour wires is typical made of low-alloyed steel, with a high yield strength in order of 700-1500MPa, depending on sour or non-sour conditions.

1.2 Inner and outer liner

Layer 2 and 9 in figure 2 is the inner and outer liner of the pipe. These layers are providing sealing of internal and external fluid to reach the pipe annulus. These layers are typical made by specific grades of polyethylene (e.g. HDPE, XLPE), or polyamide (e.g. PA11) and polyvinylidene fluoride (e.g. PVDF) [6]. The importance of these is layers is that they withstand high strain values and high bore temperatures. The temperature properties of these layers is often a limitation in flexible riser design.

1.2.1 Additional layers

In some cases, additional layers is required. These layers could be [6];

- anti-wear layers
- intermediate sheath layers
- thermal insulation layers

The most used additional layer is the anti-wear layer, the purpose of this layer is to separate the metallic armour layers, and to minimize the friction. They are typically made of the same material as the outer and inner liner.

1.3 Riser configurations

Flexible risers could be installed in several different riser configurations, figure 5. The choice of the riser configurations depends on factors such as depth, sea states, cross sectional properties, cost, etc. The most typical configurations are illustrated in figure 5.

Free-hanging catenary

The simplest configuration is the free-hanging catenary. Due to a minimum of needed subsea infrastructure it is also the cheapest one. The free-hanging catenary has poor dynamic properties and a severe amount of the vessel motion is taken up in the touch down area. The touch down point is simply



lifted off or lowered down on the seabed, and it's likely to suffer from compression buckling under high vessel motions[Bai2005]. Also, in deep water this configuration will suffer from high top tension.

Lazy wave and steep wave

In these wave configurations, buoyancy elements, made by synthetic foam, is mounted on a longer length of the riser. This will create a negative submerged weight and create the wave shape illustrated in figure 5. This will decouple the vessel motion from the touch down point (TDP) of the riser. Since the steep wave requires a subsea base and a subsea bend stiffener and the lazy wave are not, therefore the lazy wave is more often preferred. But in cases where the internal pipe fluid density changes during the lifetime of the riser, the steep waves is needed. One problem with wave-configuration is that the buoyancy elements tends to lose volume under high pressure, resulting in a increased submerged weight. The riser configuration have to be designed to accommodate up to a 10% loss of buoyancy [3].

Lazy S and steep S

In the S-configurations a subsea buoy, either fixed or floating, is connected to the pipe to create the S-shape. Here the buoy absorbs the tension variation from the vessel, and the TDP have only small variation in tension if any. The S configuration is the most expensive one, due to the needed infrastructure and are only used if a complex installation is required.

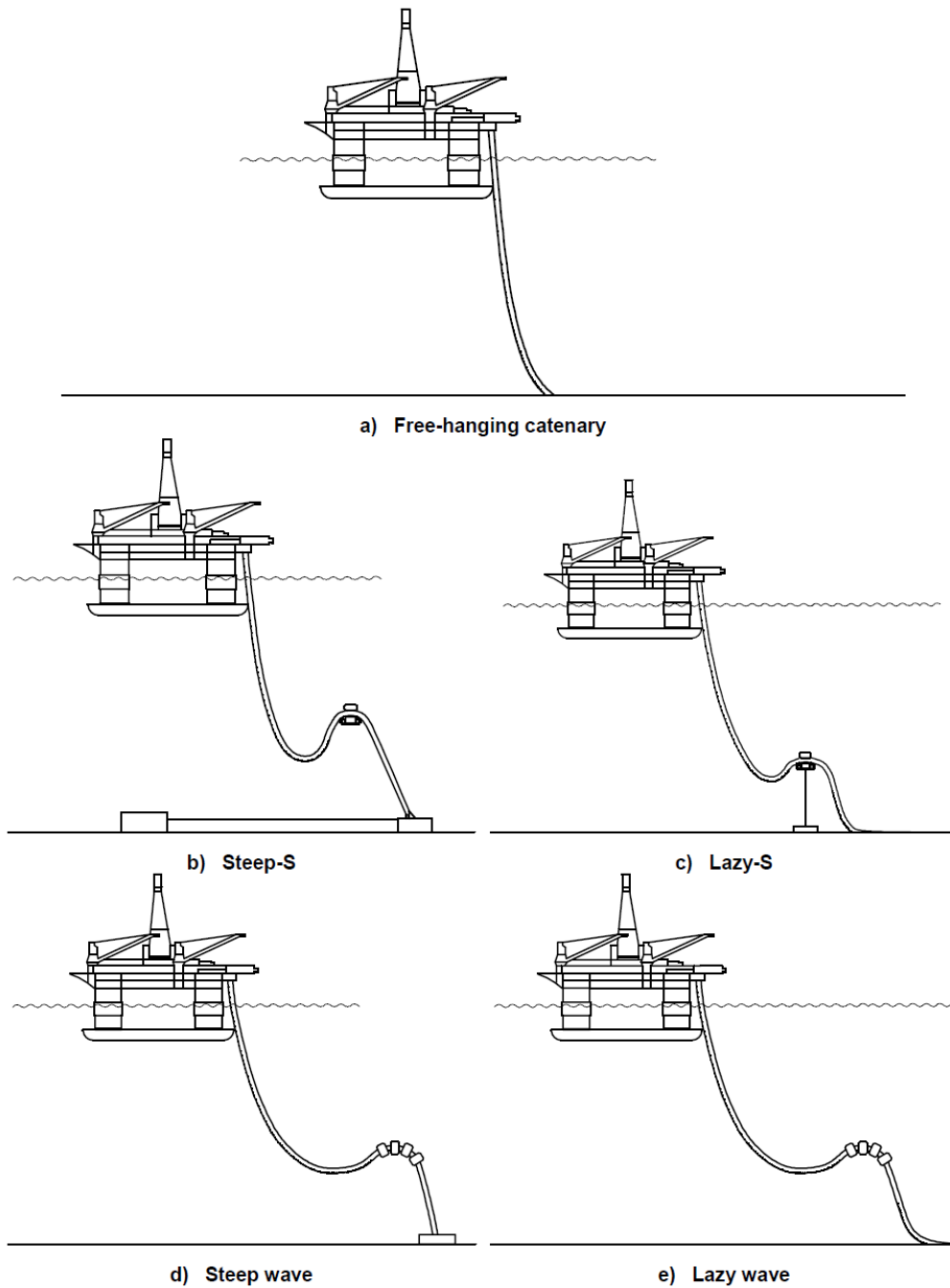


Figure 5: Riser configurations [2]

1.4 Termination of riser

One of the most critical areas of the flexible riser is at the termination point at the top of the riser. Here the riser is prone to over bending and it is therefore an interest to limit the bending curvature in this location. In general there is two ways to do this, either use a bending stiffener or a bellmouth. The bending stiffener is used to increase and distribute the pipe bending stiffness in critical areas, like termination points. The bending stiffener is typical made by polyurethane material and shaped so it's provides a gradual increase of the stiffness as it enters the hang of location, schematically illustrated in figure 6.

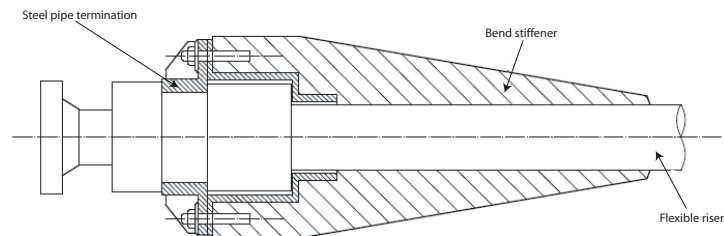


Figure 6: Schematic illustration of a bending stiffener [2]

The bellmouth does not increase the bending stiffness of the pipe, instead it is designed so it will limit the pipe curvature when the pipe is in direct contact with the bellmouth wall.



1.5 Design requirements

In flexible riser design, there is published several guidelines, RP, Specifications, to ensure that good quality of the design. Design requirements provided by the American Petroleum Institute (API) for flexible pipeline design are given in table 2.

Table 2: Flexible pipe design criteria [1]

Flexible pipe layer	Design criteria	Service conditions			Installation		Hydrostatic pressure test — FAT and field acceptance
		Normal operation		Abnormal operation	Functional and environmental	Functional, environmental and accidental	
		Recurrent operation	Extreme operation				
		Functional and environmental	Functional, environmental and accidental	Functional, environmental and accidental			
Internal pressure sheath	Creep	The maximum allowable reduction in wall thickness below the minimum design value due to creep in the supporting structural layer shall be 30 % under all load combinations.					
Internal pressure sheath	Bending Strain	The maximum allowable strain shall be 7,7 % for PE and PA, 7,0 % for PVDF in static applications and for storage in dynamic applications, and 3,5 % for PVDF for operation in dynamic applications. For other polymer materials, the allowable strain shall be as specified by the manufacturer, who shall document that the material meets the design requirements at that strain.					
Internal carcass ^a	Stress bucking load ^b	$[0,67] \text{ for } D_{\max} \leq 300 \text{ m}$ $\left[\left(\frac{D_{\max} - 300}{600} \right) \times 0,18 + 0,67 \right] \text{ for } 300 \text{ m} < D_{\max} < 900 \text{ m}$ $[0,85] \text{ for } D_{\max} \geq 900 \text{ m}$					
Tensile armours	Stress ^c	0,67	0,85	0,85	0,67	0,85	0,91
Pressure armours	Stress	0,55	0,85	0,85	0,67	0,85	0,91
Outer sheath	Strain	The maximum allowable strain shall be 7,7% for PE and PA. For other polymer materials the allowable strain shall be as specified by the manufacturer, who shall document that the material meets the design requirements at that strain.					
^a For mechanical loads the permissible utilization of the internal carcass shall be as specified for the pressure armours. ^b D_{\max} is the maximum water depth including tidal and wave effects. ^c The design criterion for the pressure and tensile armours is permissible utilization as defined in 6.3.1.4.							

2 Mechanical description

The stress obtained in the tensile armour under bending and tension is assumed to be uncoupled, hence the flexible pipe could be described by the following models [12].

- Axis-symmetrical loads due to effective tension, internal/external pressure and torsion moment
- Bending loads

The models are discussed in the following subsections and illustrated in figure 7. Most of the equations given in the following sections are taken from the FPS2000 handbook [4].

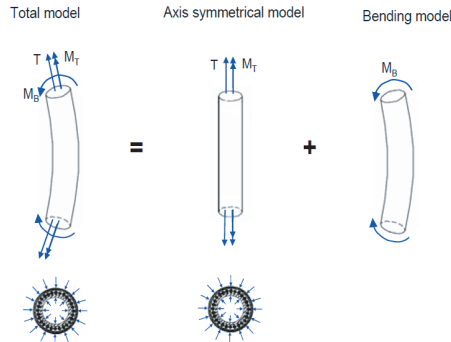


Figure 7: Response models for cross-sectional analysis [12]

2.1 Axis-Symmetrical loads

Most of the axial loads are carried by the helically wound tensile armours, and some are transferred to an inward radial force which is analogous to the external pressure. For an flexible pipe subjected to an axial force (T_e), with a given lay angle (α) for the tendons, like illustrated in figure 8, the true pipe wall force is defined as

$$\sum_{i=1}^{N_a} n_i \sigma_j A_i \cos \alpha_i = T_W = T_e + \pi p_{int} r_{int}^2 - \pi p_{ext} r_{ext}^2 \quad (2.1)$$

where n_i is the number of tendons in layer i , σ_i is the stress in the tendons from layer i , A_i is the cross section area of one tendon, p_{int}, p_{ext} is internal and external pressure and r_{int}, r_{ext} is the internal and external pressure

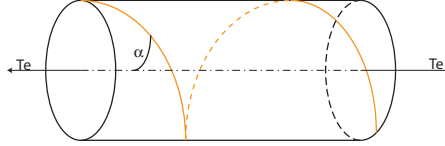


Figure 8: Flexible pipe subjected to axial force

radius. From this formula, the axial stress for a pipe with i numbers of cross wounded tensile armours could be expressed as

$$\sigma_{ta} = \frac{T_W}{\sum n_i A_i \cos \alpha_i} \quad (2.2)$$

It is seen here that the cross wounded pressure armour just give a small contribution to the pipe axial strength, since $\alpha \approx 90$ deg

2.2 Bending loads

Bending is one of the most significant properties of a flexible riser, compared to ordinary steel catenary risers. The complex way the layers interact with each other gives a hysteresis relationship between moment and curvature, as illustrated in figure 9. This curve could be described by a internal slip mechanism from the tensile armours when the pipe is exposed for bending. When the curvature is small, slip is prevented by the internal friction force between the layers, resulting in a high initial bending stiffness. To get the tendons to slip, the bending moment has to overcome the friction moment of the pipe, M_f . When slip occurs, the bending stiffness drops significantly, and the main stiffness contribution comes from the sheath layers. The friction moment depends on the contact pressure obtained from the external and internal pressure.

If the pipe is bended further then a certain limit, over bending occurs. This happens when the interlocking or helical elements interfere or touch each other, and it is often donated as the critical curvature of the pipe κ_c . When this occurs, the pipe may suffer from local buckling [4]. In a design case the critical curvature is donated as the minimum bend radius (R_{min}), where safety factors is given for different applications. In dynamic applications the minimum bending radius is typical within this range, $R_{min,d} \approx (8 - 12)d_{ext}$ [4].

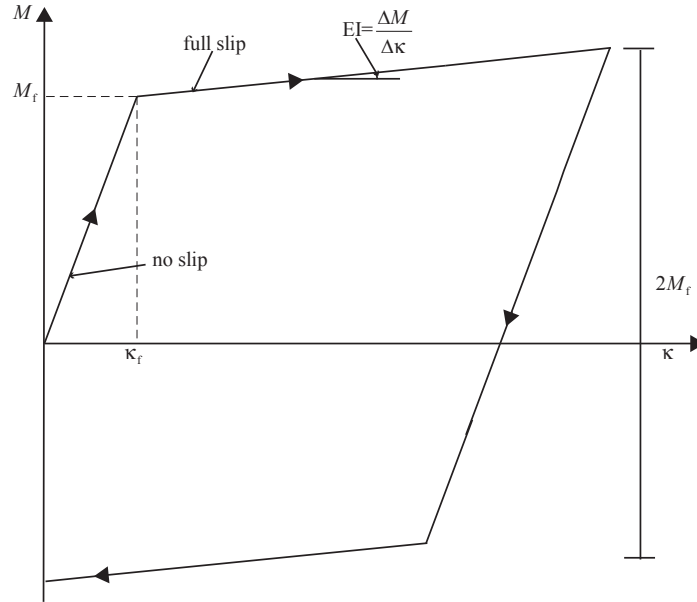


Figure 9: Bending behavior of flexible pipe

Stresses due to bending

The stress due to bending consist of two components, a static and an additional dynamic part. Due to the mean curvature (κ_m) the static stress is

$$\sigma_{tb} = \frac{3}{2}tE\kappa_m \cos^2 \alpha \cos \theta \quad (2.3)$$

The dynamic stress part, due to change of the curvature around the mean value is

$$\Delta\sigma_{tb} = \pm \frac{3}{2}tE\Delta\kappa \cos^2 \alpha \cos \theta \quad (2.4)$$

Where t is the thickness of the tendon, E is the young modulus of the material and θ is defined as cross sectional angle position of the tendon, as illustrated in figure 10

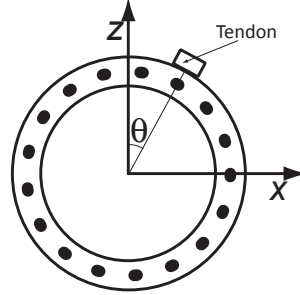


Figure 10: Definition of tendon position (θ)

Stresses due to friction

Regarding figure 10, slip will not occur at the upper surface ($\theta = 0$) and the lower surface ($\theta = \pi$). This will result in an alternating force at these points due to the sum of friction force obtained from the full slip region of the pipe ($\frac{\pi}{4} < \theta < \frac{3\pi}{4}$) and ($\frac{5\pi}{4} < \theta < \frac{7\pi}{4}$) [4]. The alternating stress due to the force at these points is expressed as.

$$\Delta\sigma_{tf} = \pm \sum (p_c f) \frac{r}{t \sin \alpha} \left(\frac{\pi}{2} - \theta \right) \quad (2.5)$$

Where p_c is the contact pressure, f is the friction coefficient and the sum sign (\sum) indicates that it is stress contribution due to friction for both sides of the tendon. The contact pressure is obtained from the axis-symmetric model and defined as.

$$p_c = \frac{\sigma_{ta} A_t \sin^2 \alpha}{R_1 t} \quad (2.6)$$

where R_1 is the radius from the inner tensile layer.

The total stress could then be found from the sum of all contributions, axis-symmetric and bending model.

$$\sigma_t = \sigma_{ta} + \sigma_{tb} + \Delta\sigma_{tb} + \Delta\sigma_{tf} \quad (2.7)$$



3 Fatigue analysis

When a material is exposed for cyclic loading, even if this load is significant smaller than the yield limit of the material, it tends to do a small amount of damage (crack growth) for each cycle. When the sum of the cyclic damage has overcome a certain limit it will result in loss of integrity, and the construction will not be able to withstand normal loading conditions. A typical cycle limit, before loss of integrity in offshore structures, is in the order of 10^8 cycles or 20 years of service time [5].

Fatigue analysis is not an exact science, it's based on imperial testing results and many assumptions has to be made. Several companies, such as Det Norske Veritas (DNV) and American Petroleum Institute (API), has published rules or recommended practices (RP) on how to perform fatigue limit state (FLS) analysis.

3.1 The SN-approach

One of the most used method to perform FLS analysis is the stress-life (SN) approach. This method is based on experimental data from fatigue tests. The results of these tests is given in SN-curves or Wöhler curves and presented in publications such as DNV's DNV-RP-C203.

The SN-curve represent the relationship between stress range and cycle limits. The basic SN-design curve is presented in equation 3.1 and illustrated figure 11 [17].

$$\log N = \log \bar{a} - m \log \Delta\sigma \quad (3.1)$$

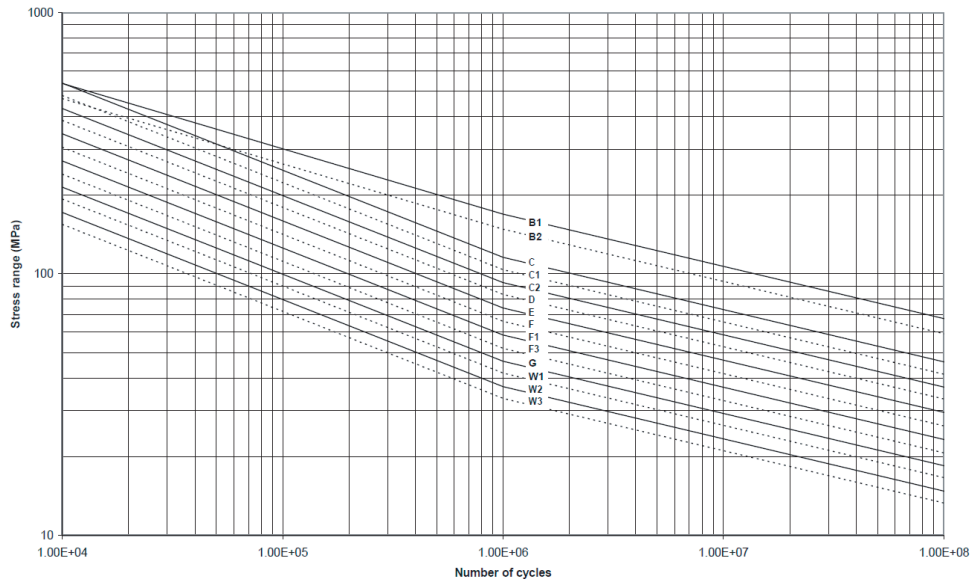


Figure 11: SN-curves in sea water with cathodic protection [17].

Here N is representing number of cycles, $\bar{\sigma}$ represent the interception of mean S-N curve with the $\log N$ axis, m represent the negative slope of the curve and $\Delta\sigma$ represent the stress range. Values for m and $\bar{\sigma}$ is given in the RP for different cases, and value for $\Delta\sigma$ has to be found from analysis etc..

3.2 Cycle counting

To perform an FLS analysis it's important to establish an sufficient cycle counting method. There is a wide range of common methods used for cycle counting, and they may differ in efficiency. The importance here is to give an good representation of the global loading, with out suffering from loss of data. One important factor for choice of counting method is the band of the load history, mainly divided into narrow band and broad band. For narrow banded series most of the counting methods yields similar results, but for broad banded series, where large cycles is interrupted with smaller cycles with a varying mean level, the cycle counts may depend significantly on the counting method [5]. Two typical counting methods are discussed in the following sections.

3.2.1 Peak counting

Peak counting is an counting technique where peaks are counted above and valleys are counted below the mean level. It may also be done without taking the mean level into contribution, counting all peaks and valleys. The peaks and valleys are then combined to create the largest possible cycle, and then the seconds largest cycle and so on. An example of peak counting is illustrated in figure 12 and the counting results is listed in table 3. It's

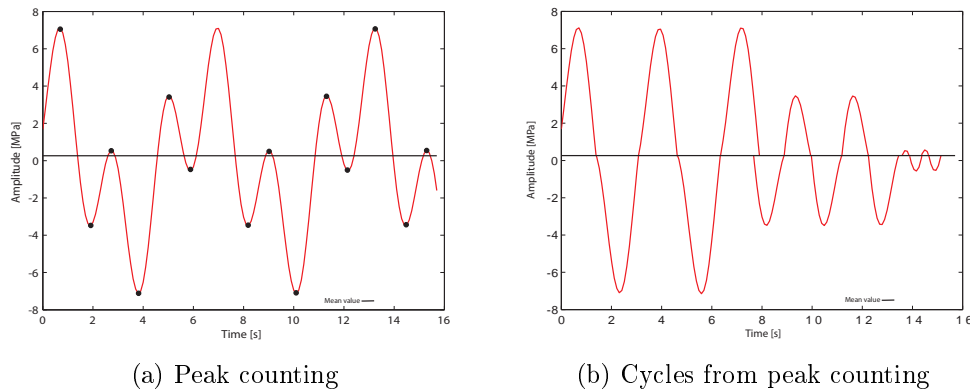


Figure 12: Peak counting of a narrow banded load history

Table 3: Results from peak counting

Stress range	Cycles
14	2.5
7	2.0
1	2.0

seen here that this counting method gives an good representation of the load history. One thing to put in mind is that all peaks where above and all valleys where below the mean level, if this was not the case the result will be different.

3.2.2 Rainflow counting

One other counting technique and one of the most used is the rainflow counting, also known as the pagoda roof rainflow counting. The name of this counting method describes the counting algorithm very well, namely rain falling down from the roof.



The rules of rainflow counting are as follows [5]:

1. Rain will flow down the roof initiating at the inside of each peak or valley. When it reaches the edge it will drip down.
2. The rain is considered to stop, and a cycle is completed, when it meets another flow from above (from the left).
3. Starting from a peak, the flow also stops when it comes opposite a more positive peak than that from which it started. Starting from a valley, the flow stops when it comes opposite a more negative valley than that from which it started.

From these rules, an example of rainflow counting is given in figure 13 and table 4.

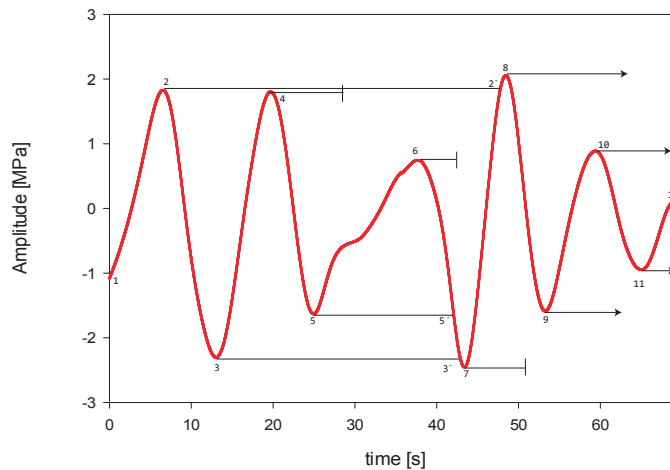


Figure 13: Rainflow counting of an broad banded load history

Table 4: Results from rainflow counting

Stress range	Cycles
4.3	2-7-2'
4.1	3-4-3'
2.4	5-6-5'
-	Half cycles
-	1-2-8

It's seen here that rainflow counting works well for a broad banded load history, and it represent cycles within bigger cycles in a good way.

3.3 Accumulated damage

The SN-curve represent a fatigue damage under constant cyclic loading, this is not the case under environmental loading. Irregular sea state will create loading cycles with a varying amplitude. The loading could be described with a load spectra, and two typical loading shapes for offshore constructions are given in figure 14 [5]. With this in mind, the fatigue

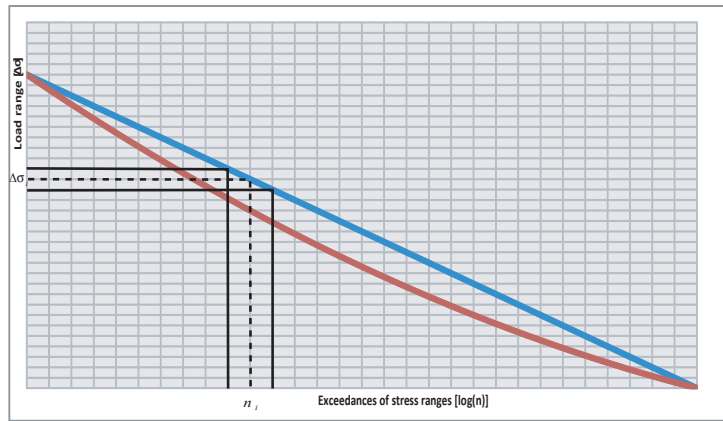


Figure 14: Illustration of typical two different offshore load spectra

analysis has to be done over several blocks with constant amplitude loading. The number of blocks should be large enough to have a good representation of the load history, and should not be less than 20 blocks [17]. By using the SN-approach for each of these blocks the accumulate damage (D) could be found. One technique often used is the Miner-Palmgren rule, described in equation 3.2 [17].

$$D = \sum_{i=1}^k \frac{n_i}{N_i} = \frac{1}{\bar{a}} \sum_{i=1}^k (\Delta\sigma)^m \leq \eta \quad (3.2)$$

Here i represents the block number, k total number of blocks, N_i number of cycles before failure for stress range i , n_i is the number of cycles in block i , \bar{a} represent the intersection of the log N axis, m represent the negative slope of the curve and η is the usage factor or inverse Design Fatigue Factor (DFF). The total design lifetime could then be expressed as

$$L = \frac{1}{D \times DFF} \quad (3.3)$$

where L is number of spectral periods the structure could resist, typical in years.



3.4 Fatigue analysis for flexible risers

Flexible pipes are complicated structures, particularly from a fatigue point of view. There is therefore given guidelines [9], RP [2] and specifications [1] to perform such analysis. Regarding API's specifications 17J, fatigue analysis should be performed for both tensile and pressure armours. When performing fatigue analysis for flexible risers it is recommended to use the following guidelines [9] from the joint industry project (JIP).

1. Global fatigue analysis of the riser system
2. Transposition from global to local analysis
3. Local stress analysis of tensile armour wires
4. Estimation of fatigue life

These are in general applied for tensile armour wires and may also be utilized for the pressure armours.

For a flexible riser it's defined global hotspots, areas typical suffering from fatigue. Mainly the hotspot is located at the riser hang of, bend stiffener area, but it may be important to include hotspots at the touch down point and at the hog and sag region of the configuration. From these locations global results should then be transposed to local model, either by a *Tension-Angle Transposition* or a *Tension-Curvature/Moment Transposition* [9]. For tensile armour the fatigue mechanism starts when the tensile tendons starts sliding against each other. The fatigue cracks are typical nucleated at the stick/slip interface, primarily from the friction force transmitted from the stick regime [4]. In a local design point of view it is defined one local hotspots for each corner of the tendons.

From a fatigue design point of view, fatigue analysis for dynamic risers should be performed with $DFF=10$. Resulting in a required lifetime of 200 years for a wanted 20 years service time.



4 Software theory

In this section discussions of SIMLA and BFLEX is performed, and most of the literature is referred to the SIMLA- and BFLEX2010- theory Manuals [13] [14]. There is not any in depth study of the principles used in the software, but basic formulations and assumptions that is important regarding the thesis is discussed here.

4.1 SIMLA

SIMLA is a FEM based computer program for static and dynamic analysis of umbilical like structures. It's mainly used for pipe laying and routing optimization, but able to solve most of pipeline engineering problems. It was started developed in September 2000 after an request from Norsk Hydro, regarding simulation of the pipeline installation at the Ormen Lange Field.

4.1.1 System structure

The SIMLA package is build up by:

- **Input files** The SIMLA input files (.sif) defines the whole model and its analysis sequence. Typically it's divided into two parts, one static initiation sequence and then one dynamic sequence. This could be done in several ways, but one way is to use two input files, one initiation file and one dynamic restart file.
- **SIMLA** Performs the FEM analysis of the model described in the input file, the results and visualization is stored in a binary .raf-file, and the dynamic time series is stored in a binary .dyn -file. These results files could be viewed in the software XPOST.
- **SIMPOST** The post processing of the FEM analysis is done in SIMPOST, here a wide range of options be processed and stored in ASCII .mpf-files. These files could ether be plotted in MatrixPLOT or open as an text file.
- **DYNPOST** Very similar to SIMPOST, but in DYNPOST the dynamic results is post processed and stored in ASCII .mpf-files.
- **HLA** HLA is the pipe laying part of SIMLA and the results is available through the SIMVIS environmental and not in XPOST.

A chart on how the different files and softwares are connected is illustrated in figure 15.

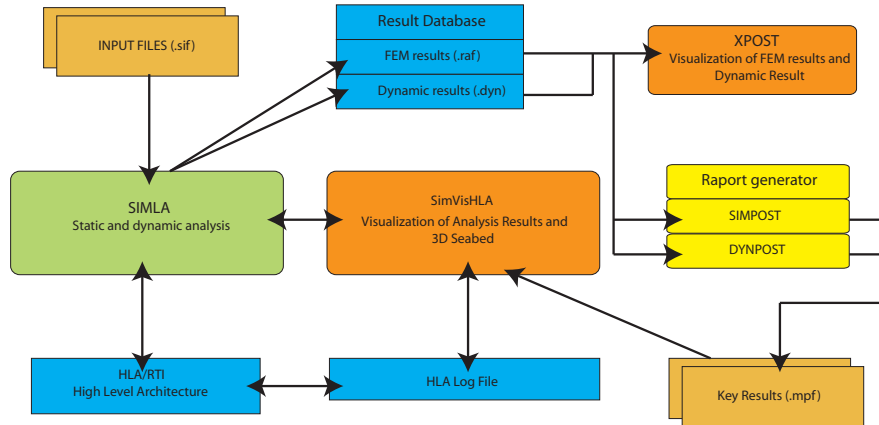


Figure 15: SIMLA system architecture

4.1.2 Principle of virtual displacement

The most frequently way to solve FEM-analysis it to use the principle of virtual displacement, or principle of virtual work. The method could be used in all kinds of one-dimensional, two-dimensional and three-dimensional structural problems. The first step here is to assume a displacement pattern between two known displacement values at the elements ends, this pattern may be a linear interposition, or any higher order depending on how good it represents the real problem. The external and internal work is then defined, and set to be equal to create an total equilibrium. In general this equilibrium is given as (excluding volume forces)

$$\int_V (\rho \ddot{\mathbf{u}} - \mathbf{f}) \cdot \delta \mathbf{u} dV + \int_V (\boldsymbol{\sigma} - \boldsymbol{\sigma}_0) : \delta \boldsymbol{\epsilon} dV - \int_S \mathbf{t} \cdot \delta \mathbf{u} dS = 0 \quad (4.1)$$

where ρ is the material density, $\ddot{\mathbf{u}}$ is the acceleration field, \mathbf{f} is the volume force vector, $\boldsymbol{\sigma}$ is the Cauchy stress tensor and $\boldsymbol{\sigma}_0$ is the initial stress tensor, $\boldsymbol{\epsilon}$ is the natural strain tensor, \mathbf{t} is the surface traction and \mathbf{u} is the displacement vector. In SIMLA all quantities are referred to initial C_0 configuration and therefore the 2nd Piola Kirchoff stress tensor (\mathbf{S}) and the Green strain tensor (\mathbf{E}) are used.



Two solve systems with large deformation and with un linearities, it has to be solve on a incremental form. There is two formulations widely used, these are Total Lagrangian (TL) and Updated Lagrangian (UL). The difference between these two formulations is the choice of reference configuration. In TL all variables are referred to the initial configuration (C_0) and for UL the variables are referred to the last obtained equilibrium configuration (C_n).

Looking at the general virtual work equation and on the incremental form, there are some needed “rules” to perform the element equations on an numerical form, these are.

- Kinematic description, i.e. a relation between the displacement and rotations and the strains at a material point.
- A material law connecting the strain with resulting stresses.
- Displacement interpolation, describing the displacement and rotation fields by a number of unknowns on matrix format.

4.1.3 Static analysis

The general static relationship between loads (\mathbf{R}) and nodal displacement (\mathbf{r}) is defined as

$$\mathbf{r} = \mathbf{K}^{-1}\mathbf{R} \quad (4.2)$$

where \mathbf{K} is defined as the global stiffness matrix of the system. For non-linear cases this has to be solve incremental, and one technique often used and used in SIMLA is the updated Newton-Raphson method. Here it is run equilibrium iterations for incremental each load step, for an one degree of freedom system this is illustrated in figure 16.

Where the load increment ΔR is given from the equilibrium state I given by load R^I to equilibrium state II given by load R^I , this is resulting in displacement increment Δr at iteration 0. The internal load vector and stiffness matrix is then updated and iteration is repeated until convergence has obtained, $\delta r_i = 0$. The total procedure could be written as

$$\Delta r_{k+1}^i = \mathbf{K}_{T,k+1}^{-1i} \Delta R_{k+1}^i \quad (4.3)$$

4.1.4 Dynamic analysis

The general forced motion equation is defined as

$$\mathbf{M}\ddot{\mathbf{r}} + \mathbf{C}\dot{\mathbf{r}} + \mathbf{K}\mathbf{r} = \mathbf{Q}(t) \quad (4.4)$$

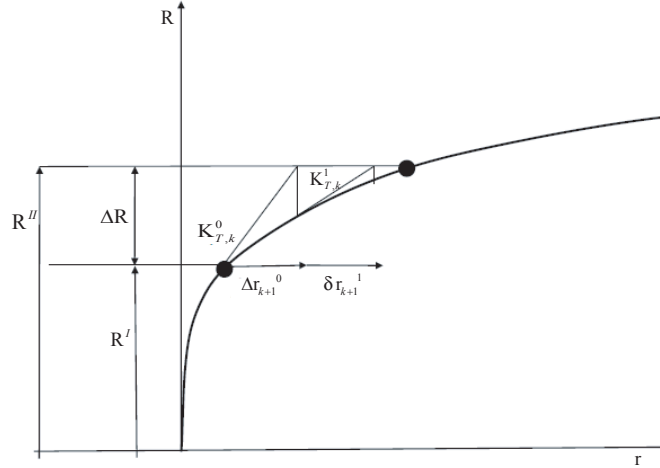


Figure 16: Newton-Raphson iteration

where \mathbf{M} is the global mass matrix, \mathbf{C} is the global damping matrix, \mathbf{K} is the global stiffness matrix and $\mathbf{Q}(t)$ is the global load vector. To perform an dynamic analysis direct time integration is necessary. This could be performed either by an explicit method, defined in equation 4.5, or an implicit method, defined in equation 4.6.

$$r_{k+1} = f(\ddot{r}_k, \dot{r}_k, r_k, r_{k-1}, \dots) \quad (4.5)$$

In the explicit method the displacement at next step will be determinate based only on information from the current time step and previous steps. The explicit method is conditionally stable, and therefore very small time steps are required. For impulse analysis, where it's needed small time steps to achieve sufficient accuracy, this method is a good choice.

$$r_{k+1} = f(\ddot{r}_{k+1}, \ddot{r}_k, \dot{r}_{k+1}, \dot{r}_k, r_k, \dots) \quad (4.6)$$

In the implicit method the displacement at the next time step depends on quantities at the next time step, together with information from the current step. Since the implicit method use information from the next step, this method have better numerical stability than the explicit method. To use information from the next step an assumption on how the system accelerate between the time steps has to be done. Some basic examples are the constant average acceleration, linear acceleration and the constant initial acceleration [11]. Often there is used the Newmark- β with different λ - and β -values to represent the different acceleration modes, depending on accuracy and stability requirement [11].



When using implicit methods is used it's necessary to solve a coupled equation system at every incremental time step, therefore this method will become time uneconomical if short time steps are unavoidable, due to accuracy.

Dynamic analysis results in a series of modes, where mostly the lower frequency modes is interesting. It's therefore desirable to remove higher modes without suffering inaccuracy in the lower modes. One option is to use higher damping ratio or introduce Raylieh damping in the Newmark- β method, but this is only removing the middle modes only and leaves the higher and lower modes untouched.

In SIMLA the HHT- α method are used for time integration of dynamic systems, it's very similar to the Newmark- β -method, but it's introduced a numerical damping without suffering from inaccuracy. The method is damping higher terms and maintain the 2nd order accuracy. The modified incremental motion equation for the system is then

$$\mathbf{M}\ddot{\mathbf{r}}_{k+1} + (1 + \alpha)\mathbf{C}\dot{\mathbf{r}}_{k+1} - \alpha\mathbf{C}\dot{\mathbf{r}}_k + (1 + \alpha)\mathbf{R}_{k+1}^I - \alpha\mathbf{R}_k^I = (1 + \alpha)\mathbf{R}_{k+1}^E - \alpha\mathbf{R}_k^E \quad (4.7)$$

where \mathbf{M} , \mathbf{C} and \mathbf{K} has the same definition as in equation 4.4, \mathbf{R}^I is the internal force vector, \mathbf{R}^E is the external force vector and α is constant witch defines the numerical damping, recommended to be $-1/3 \leq \alpha \leq 0$. In this method the damping matrix \mathbf{C} include both Rayliegh damping and diagonal damping.

4.1.5 Pipe element definition

In Simla pipe elements is defined with linear interpolation for torsion, rotation and axial displacement whereas cubic interpolation is used in the transverse direction with at total of 12 degrees of freedom, as illustrated in figure 17.

4.1.6 Material models

In SIMLA it's possible to use elastic and elastoplastic material definitions. The elastic model is defined by the general Hook's law in matrix form,

$$\boldsymbol{\sigma} = \mathbf{D}\boldsymbol{\epsilon} \quad (4.8)$$

where $\boldsymbol{\epsilon}$ is the strain vector, $\boldsymbol{\sigma}$ is the stress vector and \mathbf{D} is a matrix describing the relationship between stress and strain. This material description is sufficient small loads and displacement, where high stresses in not the case.

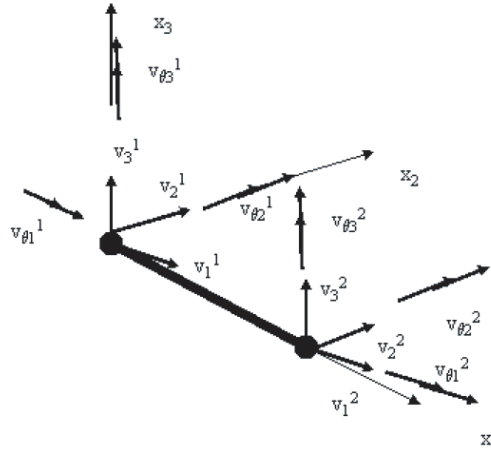


Figure 17: Pipe element in SIMLA

When the material exceeds the elastic limit of stress/strain, an elasto-plastic formulation is required and to describe the plasticity, three major features are needed;

- **A yield criterion** A criterion for defining which combinations of multi-axial stresses cause the material to be plastic.
- **A flow rule** Relating the plastic strain to the history of stress and strain and the stress rate.
- **A hardening rule** Defines the change of yield condition as the plastic flow proceeds.

4.1.7 Hydrodynamic loading

For modeling of hydrodynamic forces on pipes the Morison's formulation is applied in SIMLA. For an arbitrarily oriented, moving structures (such as risers) it's general defined as [2]

$$f_m = \frac{1}{2}\rho_w D_d C_d V_{RN} |V_{RN}| + \rho_w \frac{\pi D_d^2}{4} C_m \dot{V}_{WN} - \rho_w \frac{\pi D_d^2}{4} (C_m - 1) \dot{V}_{PN} \quad (4.9)$$

where f_m is the load per unit length V_{RN} is the normal relative fluid velocity, \dot{V}_{WM} is the normal water particle acceleration, \dot{V}_{PN} is the normal structural acceleration, D_d is the effective drag diameter, C_d is the drag coefficient, C_m is the inertia coefficient and ρ_w is the seawater density. In



SIMLA the Morrison's equation is defined in three parts, regarding tangential force in local x-direction and normal force in local y- and z-direction.

4.1.8 Wave kinematics

Regular waves

Regular waves are in SIMLA modeled by the Airy linear wave theory, and the wave potential in deep water could then be described by

$$\phi_0 = \frac{\zeta_a g}{\omega} e^{kz} \cos(-\omega t + kX \cos \beta + kY \sin \beta + \psi_\phi) \quad (4.10)$$

where ζ_a is wave elevation, g is acceleration of gravity, k is the wave number, β is the wave direction ($\beta=0$, along positive X -axis) and ψ_ϕ is the phase angle. And the surface elevation given by

$$\eta = \zeta_a \sin(\omega t - kX \cos \beta - kY \sin \beta + \phi) \quad (4.11)$$

where the same constant is used as in the wave potential equation, but here $\phi = -\psi$. One issue here is that the wave potential is valid to mean water level only and are not including velocities and acceleration at the wave crest. To solve this, SIMLA performs a integration to mean water level, where it's assumed that the water level always remain at mean water level.

Irregular waves

The irregular sea state could be described as an sum of two wave spectra; a wind sea contribution and a swell contribution, and defined as

$$S_{\zeta,TOT}(\beta, \omega) = S_{\zeta,1}(\omega)\phi_1(\beta - \beta_1) + S_{\zeta,2}(\omega)\phi_2(\beta - \beta_2) \quad (4.12)$$

where $S_{\zeta,1}$ and $S_{\zeta,2}$ defines frequency distribution for sea and swell, ϕ_1 and ϕ_2 defines the directionality of the waves (only unidirectional waves are included in SIMLA) and β is the directions of wave and swell propagation. In irregular waves the surface wave elevation is expressed as a sum of wave components

$$\eta(x, y, t) = \sum_{k=1}^{N_\omega} A_k \sin(\omega_k t + \phi_k^p + \phi_k) \quad (4.13)$$

where the component wave amplitude A_k is defined as

$$A_k = \sqrt{S_\eta(\omega)\Delta\omega} \quad (4.14)$$



S_η is the wave spectra and could either be described by the two paramatra Pierson-Moskowitz (PM) spectrum or the three parametra Jonswap spectrum. The PM-spectrum is defined as

$$S_\eta(\omega) = A\omega^{-5}e^{-\frac{B}{\omega}}, 0 < \omega < \infty \quad (4.15)$$

Where A and B is defined as

$$A = 124.2 \frac{H_s}{T_z^4}$$

$$B = \frac{496}{T_z^4}$$

where T_z is the zero crossing period and H_s is the significant wave height. The period used in most scatter diagrams is the peak period (T_p) and the relationship between zero crossing and peak period is $T_p = 1.408T_z$.

The Jonswap spectrum is given as

$$S_\eta(\omega) = \alpha g^2 \omega^{-5} e^{-\beta(\frac{\omega}{\omega_p})^4} \gamma e^{-\frac{(\omega - \omega_p)^2}{2\sigma^2 \omega_p^2}} \quad (4.16)$$

Where the constants is defined, as follows

$$\alpha = 1.2905 \frac{H_s^2}{T_z^2}$$

$$\beta = 1.205 \text{ for North Sea Conditions}$$

$$= 1.0 \text{ when } T_p > 5\sqrt{H_s}$$

$$\gamma = e^{5.75 - 1.15 \frac{T_p}{\sqrt{H_s}}}$$

$$= 5.0 \text{ when } T_p < 3.6\sqrt{H_s}$$

$$\sigma = 0.07 \text{ for } \omega \leq \omega_p$$

$$= 0.09 \text{ for } \omega \geq \omega_p$$

$$\omega_p = \frac{2\pi}{T_p} \frac{T_p}{T_z} = 1.407(1 - 0.28 \ln \gamma)^{1/4}$$

like PM-spectra, the constants T_z and T_p and H_s has the same definition.

Forced vessel motion

For flexible risers an vessel is connected in the end. Motions of this vessel is important to know under dynamic riser analysis. The motion of the vessel is then described by a set of complex transfer functions for all six degrees of freedom.



4.2 BFLEX2010

BFLEX2010, originally BFLEX, is a computer program for stress analysis of flexible pipes. It was originally developed by SINTEF Civil and Environmental Engineering as part of the project; *Service Life Analysis of Deep water Risers*. The total BFLEX2010 package consist of several analytical tools and they are listed below

- **BFLEX2010** Reads and controlling the input data given in the .2bif-file. It's then performs the global analysis as well as the tensile armour analysis, the results is then given in an .Raf-file that could be graphical viewed in XPOST.
- **BFLEX2010POST** Performs post processing of the local result into ASCII files that could be plotted by the plotting program Matrixplot, also it's generates a new .Raf-file where the results from the following modules is stored.
- **BPOST** Performs post processing of the global results, the results is stored in ASCII files that could be blotted in Matrixplot
- **BOUNDARY** Performs transverse cross-sectional stress analysis, mainly of the pressure armours. The results is stored in the post processed .raf- file.
- **PFLEX** Performs the beam stress analysis of the pressure spiral. The results is stored in the post processed .raf- file.
- **LIFETIME** Performs fatigue calculations for the pipe, where the SN-data is Vivien in a input file.

An system structure illustration is also given in figure 18.

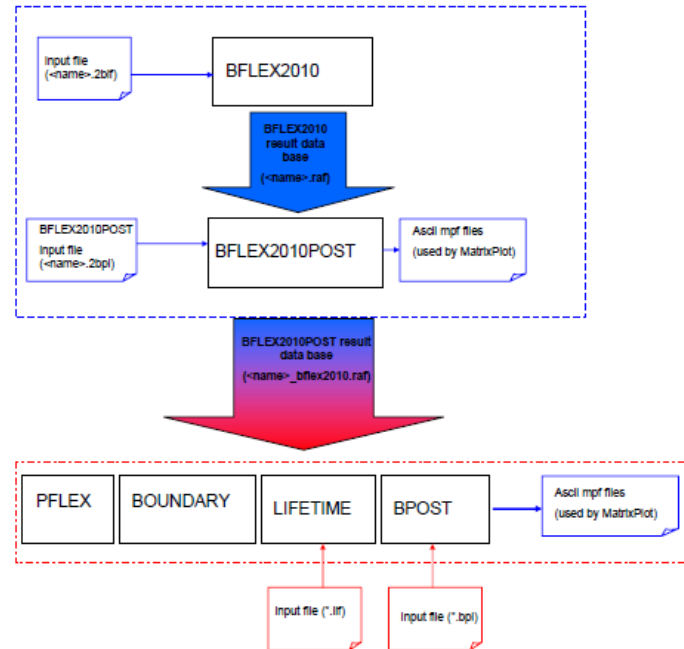


Figure 18: BFLEX2010 System structure [15]

4.2.1 Similarity to SIMLA

The principles used in Bflex2010 is very similar to SIMLA, and not discussed her. Therefore topics like dynamic and static analysis and principles of virtual displacement is referred to the SIMLA part.

4.2.2 Bending formulation

In BFLEX2010 it's represent three different bending formulations for the tensile armour, these are

- **ITCODE0** - Based on considering the equilibrium equation of each individual tendon considering the shear interaction with the core pipe, by application of Sandwich Beam formulation (SBM)
- **ITCODE21** - Based on a moment based model (MM), considering the friction moment contribution from all layers. Here only one moment-curvature curve used, where the slip curvature is based on the inner layer only.
- **ITCODE31** - Also based on a moment based model (MM), but here one moment-curvature curve is created for each layer, taking into



account the slip property of each layer. Meaning that a four layer pipe will have four moment-curvature curves with different slip levels. Regarding the result obtained, the ITCODE31 is the most accurate compared to full scale tests.

To represent a realistic stick-slip effect the moment-curvature model is divided into three regions, as following;

- **Region I** - Is the stick region, where plane surface remain plane.
- **Region II** - Is the stick-slip region, where one section is in the stick region and the other part is in the slip region. This region is defined when bending moment reach $\frac{\pi}{4}M_f$.
- **Region III** - Is the slip region, where the entire length is under slip condition.

5 Global analysis

5.1 Model description

5.1.1 Modeling of riser configuration

The riser is modeled in a steep wave configurations, as described in appendix A and as illustrated in figure 19

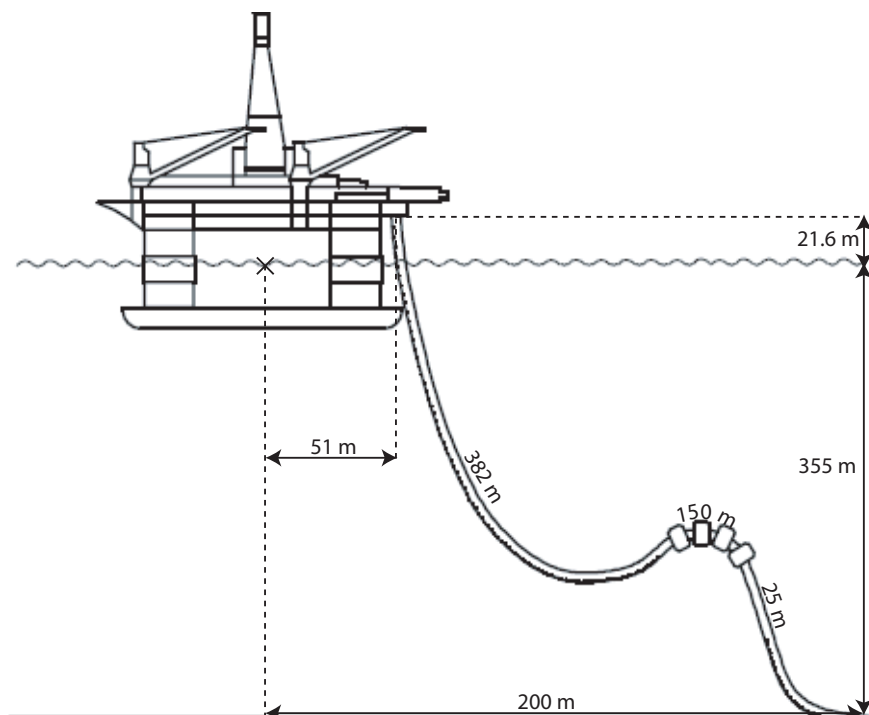


Figure 19: Dimensions of riser configuration



The main properties of the flexible riser are also given in table 5.

Table 5: Pipe properties

Property	unit	
Length	m	565.0
Diameter	mm	401.0
Dry mass pipe	kg/m	406.0
Submerged mass pipe	kg/m	272.0
Buoyancy diameter	mm	1032.0
Dry mass buoyancy	kg/m	512.0
Submerged mass buoyancy	kg/m	-400.5
Bending stiffness _{Slip}	Nm ²	2.35E05
Bending stiffness _{Stick}	Nm ²	7.00E06
Axial stiffness	N/m	6.0E08

To describe the bending hysteresis behavior of an flexible riser, it's modeled two sets of global analysis, one where the pipe has the same bending stiffness as the stick regime and one where the pipe has the same bending stiffness as the slip regime. Calculations for this regimes are done in the project thesis 2010, and it's graphical calculated in figure 20. From these calculations the friction curvature (κ_f) is found to be approximately 0.01 m^{-1} and the corresponding friction moment (M_f) is 100 kNm .

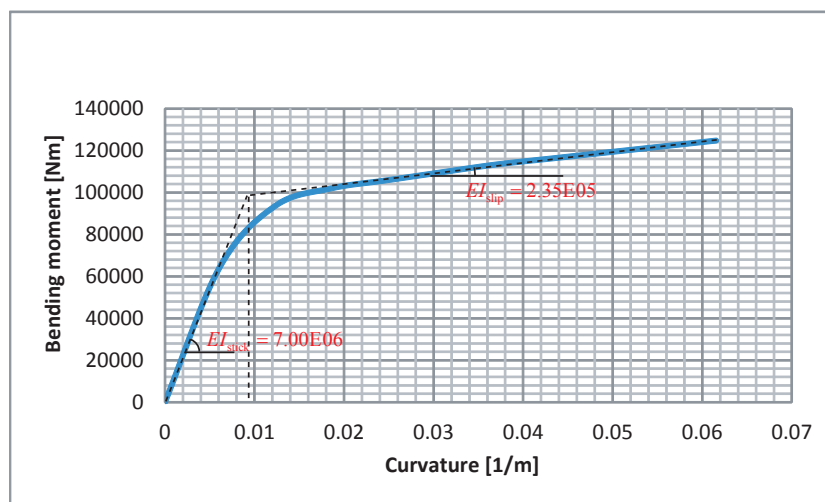


Figure 20: Bending - Curvature relationship $p_{int}=475 \text{ bar}$

Meshing and element type

The configuration is meshed up with 642 nodes, connected with 641 linear pipe elements(pipe31 [16]). The mesh size, starting from the termination point, is 0.1 to 1 meter for the first 20 meters of the riser. The rest of the elements are seeded to be 1 meter.

Boundary conditions

The riser is eccentric connected to an semi submersible with an given first order RAO for all six degrees of freedom (DOF). The riser is simple supported at the sea floor. In total there are 28 boundary conditions and 3842 equations to solve at each load step.

5.1.2 Environmental data

The analysis is performed in fully developed irregular wave condition, and therefore described with help of the two parametra PM spectra. The sea states data, H_s and T_p , is given in a omni directional scatter diagram from the Statfjord field [7]. To reduce the amount of computing time the scatter diagram is divided into 18 blocks, table 6.

Table 6: Blocked scatter diagram, Statfjord field [7]

Hs	Spectral peak period 3hrs during 34 years																		SUM													
	0-3	3-4	4-5	5-6	6-7	7-8	8-9	9-10	10-11	11-12	12-13	13-14	14-15	15-16	16-17	17-18	18-19	19-20		20+												
0-1				4155						1192			202						5548													
1-2				19605						11267			2035						32907													
2-3	0				18290						10349			728						29367												
3-4	0	0				12971						3154									16125											
4-5	0	0	0				6791						1133									7924										
5-6	0	0	0	0				3645						373									4018									
6-7	0	0	0	0	0										3154			0						0								
7-8	0	0	0	0	0	0													0						0							
8-9	0	0	0	0	0	0	0													0						0						
9-10	0	0	0	0	0	0	0	0													0						0					
10-11	0	0	0	0	0	0	0	0	0													0						0				
11-12	0	0	0	0	0	0	0	0	0	0													0						0			
12-13	0	0	0	0	0	0	0	0	0	0	0													0						0		
13-14	0	0	0	0	0	0	0	0	0	0	0	0													0						0	
14-15	0	0	0	0	0	0	0	0	0	0	0	0	0													0						0
SUM	0	0	0	0	4155	37895	0	12971	10406	12459	10349	0	0	3154	225	6524	1101	0	0	0	0	99269										

All sea states are in an conservative way propagating in the same direction, along the positive direction of the global X -axis. Wind and current loads is not taken into account under the global analysis.



5.1.3 Simulation

As stated in subsection 5.1.2 number of environmental cases is set to 18, and as also stated in subsection 5.1.1 this is done two times to represent the bending behavior. Regarding simulation length, the analysis was run in a duration of 1 hour, where the total simulation represent an average sea state of one year. The incremental time step is for most of the cases set to be 0.1 seconds, so the smallest peak periods (5.5s) get 55 storage points. However, due to numerical instability for the two most extreme load cases in slip regime the incremental time step is set to 0.05 seconds. The simulations has been run for 1 hour periods, where the first 20 seconds is used for initiation of configuration and wave build up. For the calmest sea states the compiling time was about 4-5 hours, and for the most extreme states the compiling time increased up to 12 hours. For the two cases with smaller time step the compiling time was 20 hours. The main simulation data are given in table 7.

Table 7: Simulation of cases

Number of sea states analyzed	18
Simulation duration per case	1 hour
Number of time steps per simulation	36900*
Average compiling time	8 hours
<small>*For $H_s=12.5$ and $H_s=10.5$ in the slip regime the global analysis has to be performed with a number of 72800 time steps</small>	

5.1.4 Results of interest

The results needed for global analysis is the nodal rotation about the local y-axis for node 1 (termination) and node 75 (10 meters from termination), the difference between these two values ($\Delta\theta$ -value) will be used as input for the local analysis. Also the mean effective wall tension (T_e) in node 75 will be used the local analysis. One important factor here, to be able to represent the configuration in a good way, is that the curvature is close to zero at element 75. If this is not the case, the lower pitch motion has to be collected further down the riser. The results of interest are illustrated in figure 21.

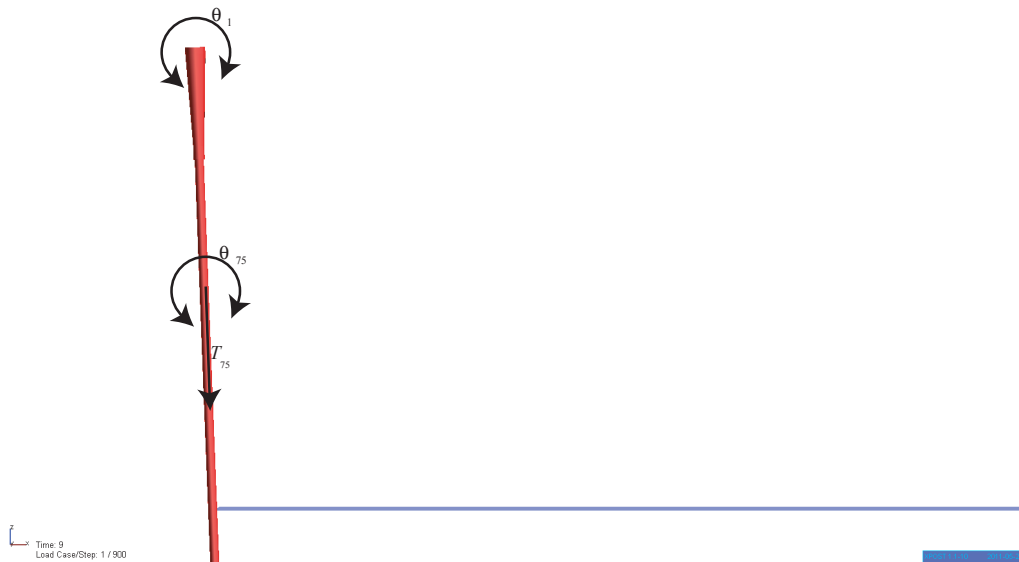


Figure 21: Results of interest

To verify the global model, regarding stick and slip limits and critical curvature, it's also necessary to look at the curvature distribution along the risers for the different sea states. In dynamic cases where the pipe has an external diameter on 401mm, the maximum curvature should not exceed 0.21m^{-1} ($R_{min,d} \geq 12D_{ext}$).

5.2 Results

The results sections is divided into 4 different parts, a static part, a slip part, a stick part and a conclusion part. Regarding the $\Delta\theta$ -values, these are obtained from 2 different dynamic series, one for each global node (1 and 75), the results is then cycle counted with help of a rainflow counter provided by Matlab. The cyclic counts are then stored into 20 blocks with a $\Delta\theta$ range of 1/3 degrees. The results plots in this section is taken from the sea state with a 12.5 meter significant wave hight and a 12.5 seconds peak period, ref. to sea state 18 for the next sections ($H_s=12.5\text{m}$ and $T_p=12.5\text{s}$)

5.2.1 Static results

On the static results parts is focused on how the configuration tends to make a sufficient wave-shape and also look at the global curvature along the riser to check what regime the pipe is in under static calm sea condition, they are both illustrated in figure 22.

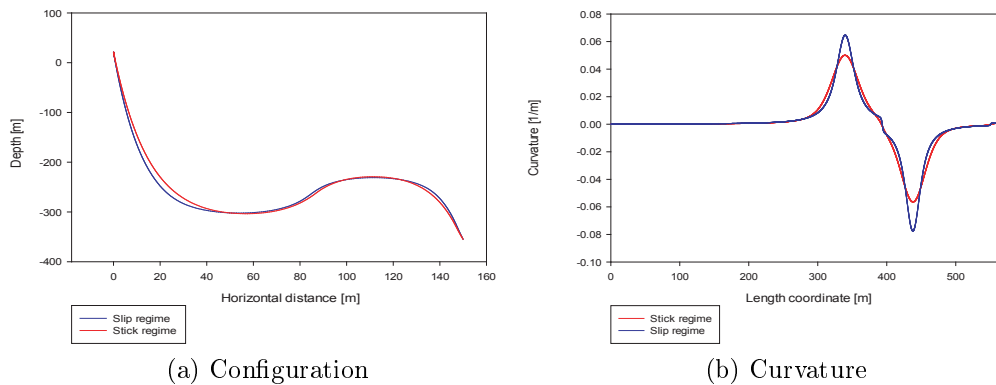


Figure 22: Dynplot series of nodal displacement in pitch

It's seen here that the shape of the global configuration looks fine and there is not any big different between the two regimes. For the curvature plot the global curvature distribution along the riser is in over the κ_f -value of 0.01 for the hog/sag region of the riser and regarding the criteria of zero curvature at 10 meters from termination point seems to be satisfied. However, this has also to be checked for the dynamic analysis. One other interesting part to look upon in the static analysis is the tension distribution along the flexible riser, this is illustrated in figure 23.

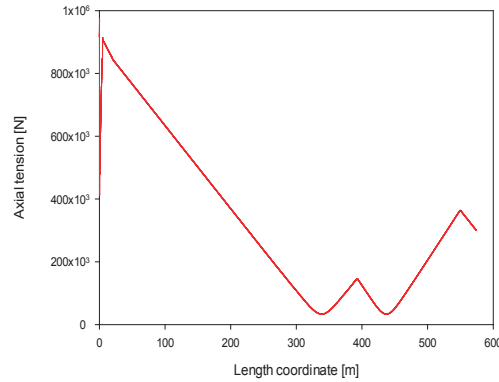


Figure 23: Static axial tension distribution along the riser length coordinates

The static tension is here $912kN$ at hang off and $880kN$ at node 75, the tension then decrease to $33kN$ at the deepest sag point in the configuration and due to the buoyancy elements it increase again to $300kN$ at the bottom. Simple calculations from the catenary equation [8] is here used to verify the top tension (T_{max})

$$T_{max} = T_H + w_d h_d + w_s d_s = 0 + 406 \cdot 9.81 \cdot 21.5 + 272 \cdot 981 \cdot 300 = 886[kN] \quad (5.1)$$

where T_H is the horizontal tension[N] , w_d and w_s is the dry and submerged weight [N/m] and h_d and h_s is the vertical length[m] for the dry and submerge part of the configuration. The result here is very similar to analytical result, due that the horizontal tension T_H is not zero in the real case.

5.2.2 Stick regime

The enveloped curvature distribution along the riser for sea state 18 in the stick regime is illustrated in figure 24

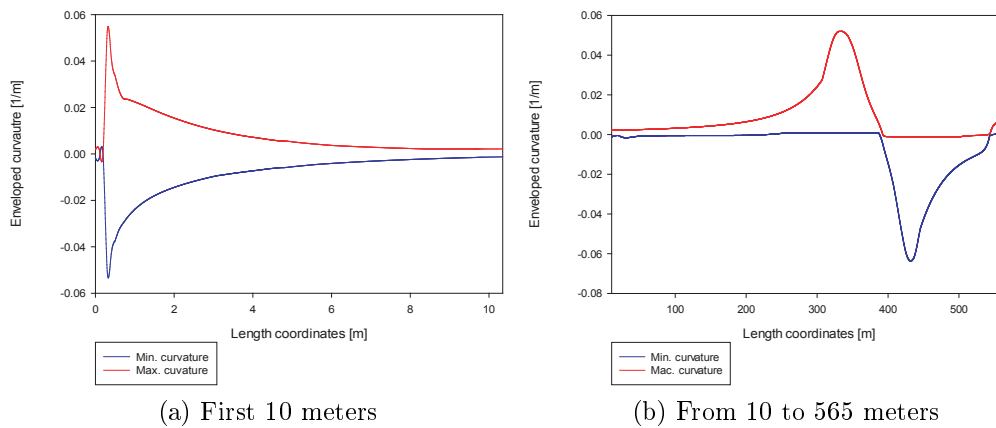


Figure 24: Enveloped curvature of riser in stick regime (Sea state 18)

For the first 10 meters segment of the riser the maximum and minimum curvature is $\pm 0.052\text{m}^{-1}$ close to the hang off location. The sudden increase at the hang off location is due to a rigid pipe needed for numerical stability of the riser. For the rest of the pipe the maximum curvature is 0.52m^{-1} in sag region, only 4% bigger than static analysis, and the minimum curvature is -0.63m^{-1} in the hog region, 10% bigger than the static analysis. In addition it's a little curvature peak of 0.006m^{-1} at the touch down point, however the configuration seems to uncouple the vessel motion very well. Regarding the demand of zero curvature at element 75 is not fulfilled here, but since the curvature here is small and it's not seemed to decrease further down the riser it's acceptable.

A part of the dynamic series of node 1 and node 75, as well the $\Delta\theta$ -series for sea state 18 is plotted in figure 25. And the result from cycle counting is plotted into figure 26

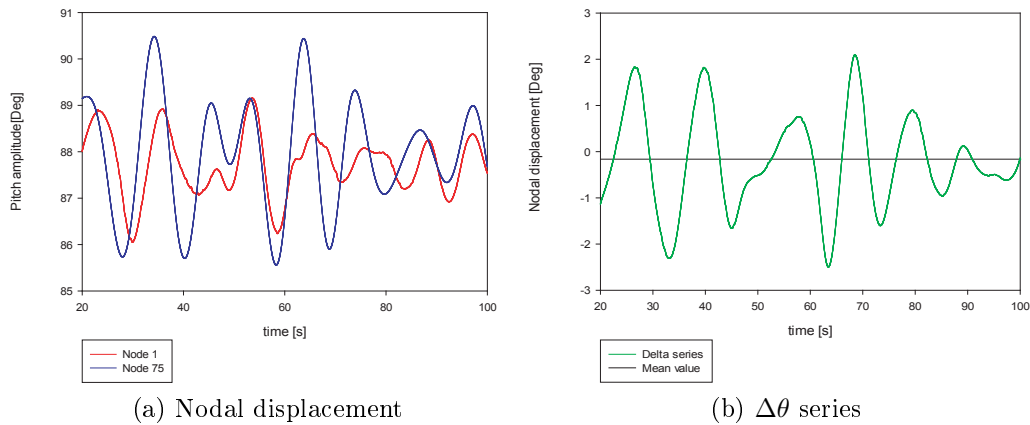


Figure 25: Dynplot series of nodal rotation about the local y-axis

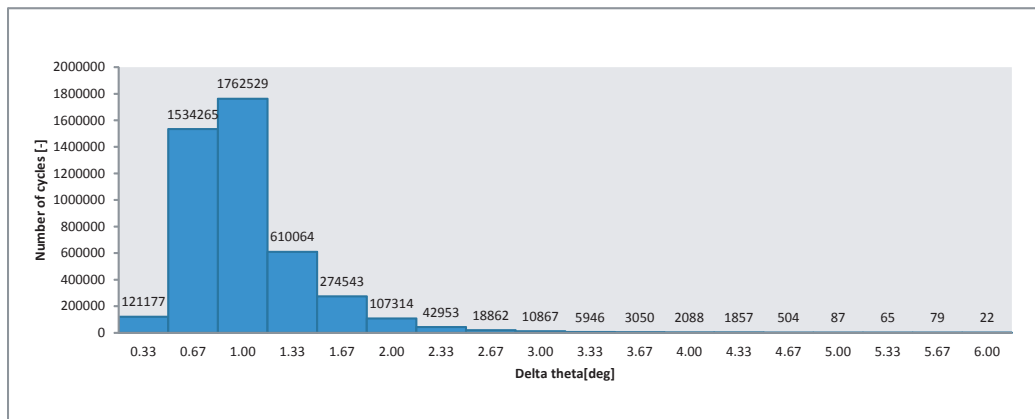


Figure 26: Load counting in stick regime

The $\Delta\theta$ series results in a negative mean value, -0.24 degrees, and could be explained by the non zero curvature obtained from element 75. From the cycle count it is seen that the median of the cycles is gathered around a $\Delta\theta$ -range of 1.00 degrees. Regarding the the typical load spectra shape illustrated in figure 14 where most cycles are assumed to belong in the first block is not the case in this load history. The total cycle counts in stick regime analysis results in an total of 4.50E06 cycles, only 50.0E05 cycles from the reference number of 5.00E6 cycles per year.

5.2.3 Slip regime

For the slip regime the enveloped curvature along the riser is plotted in figure 27. Here the enveloped curvature for the first 10 meters is by far

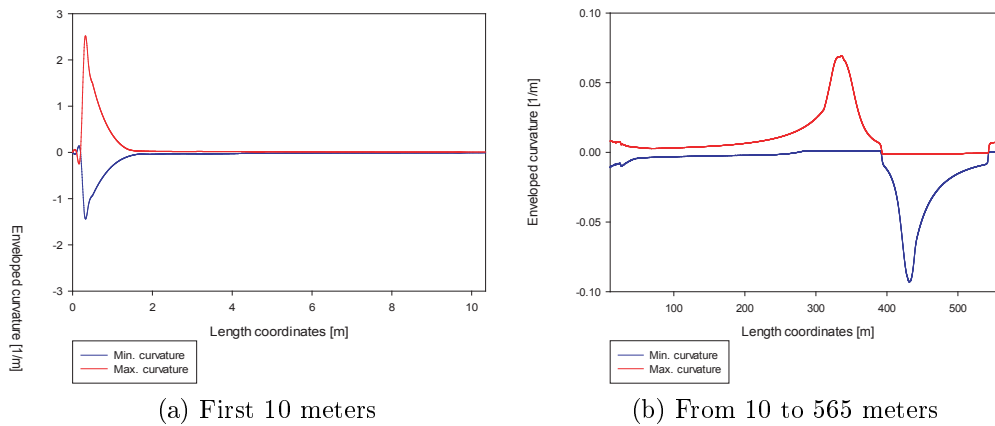


Figure 27: Enveloped curvature of riser in slip regime

larger, compared to the slip regime, also it's by far larger than the maximum allowed curvature, 0.21m^{-1} , defined in section 5.1.4. Regarding the demand of zero curvature at element 75 is also not fulfilled in this analysis, and compared to the stick regime it still decrease further down the riser. But due to discussions done later in this subsection it's chosen to be good enough.

For the slip regime the same dynamic time series as in stick regime is plotted in figure 28.

It is seen here, that specially node 1 results in a very ripple $\Delta\theta$ -series. Regarding the cycle counting this is a big issue, but with help of a Savitzky-Golay filter in Matlab this problem is taken care off. Also the high maximum curvature obtained from sea state 18 may result from this numerical issue, and therefore it is not taken into concern. Result of the smoothing is illustrated in figure 29. The results from rainflow counting is then plotted in figure 30.

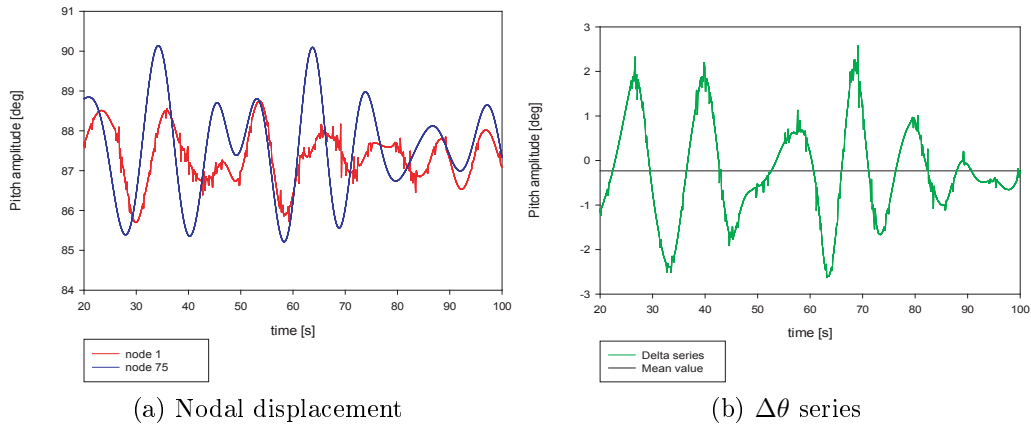


Figure 28: Dynplot series of nodal rotation about the local y-axis

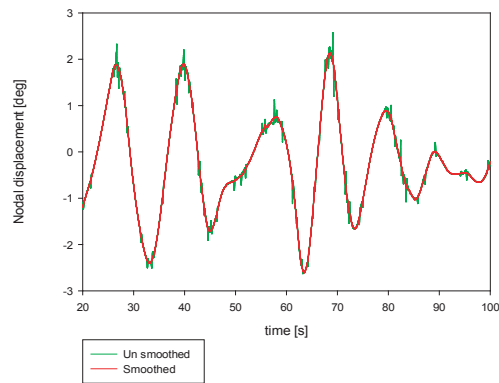


Figure 29: Smoothed response in slip regime

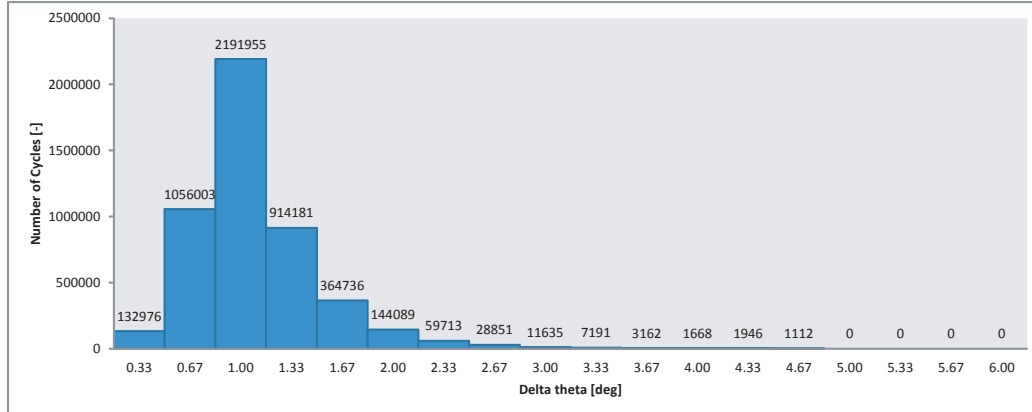


Figure 30: Load counting in slip regime

Also here $\Delta\theta$ -series results in an average negative value and a little larger than the slip regime, -0.29 degrees. Regarding the cycle counting, the average of the cycles is also gathered in the $\Delta\theta$ -range of 1.00 degrees, but the cycles seem to have been transferred in the direction of bigger cycles. But, there are only cycles counted up to a $\Delta\theta$ -range of 4.76 , and then a sudden stop. The total amount of cycles in the slip regime is $4.92E06$ cycles, and only 80800 from the reference number of $5.00E06$ cycles.

5.2.4 Conclusion

By comparing the results it's seen that the number of cycles is a little different of the regimes, the difference of total $460\ 000$ may result from some left over rippled noise in the slip regime time series. Regarding that the slip regime results in more higher $\Delta\theta$ counts is very convenient, due to the lower bending stiffness of this regime. But, it is very odd that no cycles are obtained from block 15 to 20. This may be explained by the use of the Savitzky-Golay filter, which tends to use an average value. However to conclude that dividing the analysis into two regimes is a good assumption or not is not sufficient from this global analysis.

6 Local analysis

6.1 Model description

The local model is modeled in BFLEX2010 with the cross section described in Appendix B, and illustrated in figure 31. The general pipe properties are also given in table 8.

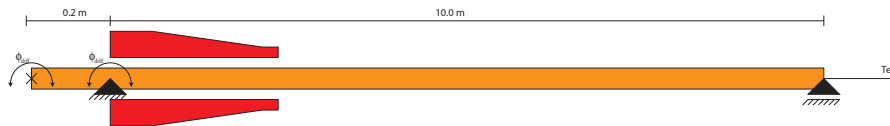


Figure 31: Local BFLEX2010 model (Not in scale)

Property	Units	[-]
Ext. pipe diameter	mm	401.0
Int. pipe diameter	mm	228.6
Pipe length	m	10.2
Internal pressure	MPa	47.5
Number of layers	-	20
Tensile armours	-	4
Pressure armours	-	2

Table 8: Pipe properties

Meshing and element

The pipe itself is meshed up with 205 global nodes, with a constant space of 50mm between them. The pipe consist of 5 layers, four layers representing the four tension layers, and one core layer representing the rest of the pipe. Each layer is divided into 204 elements, resulting in a total of 1020 pipe elements. Part of the model with meshing is illustrated in figure 32.

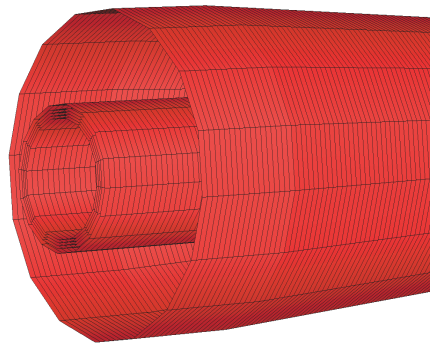


Figure 32: Mesh of BFLEX2010 model

Constraints and boundary conditions

The model is modeled up like a simply supported beam, with 3 active constraint equations, reffered to figure 31. To represent an rigid motion from the vessel there is used 2 equations to describe the $\Delta\theta$ -series obtained from the global SIMLA analysis, active on node 1 and 5. The θ -constraint is illustrated in figure 33 and also discussed in section 6.1.3

The last equation describes the effective mean wall tension obtained from the global analysis, active at node 205. To save computational time, unnecessary degree of freedom are removed along the whole pipe, these are rotation about local x-axis and z-axis and displacement in local y-axis.

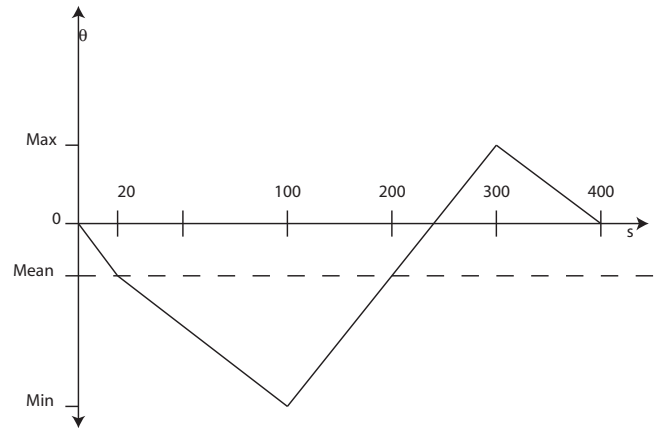


Figure 33: θ -series constraint

6.1.1 Bending stiffener

The bending stiffener is modeled in two different ways, these are;

- **Model 1** The bend stiffener is modeled with dependent node system, where the local bending stiffener nodes is in direct connection of the global nodes. Hence, gap investigation is not possible.
- **Model 2** The bend stiffener is modeled with independent node system, where the local bending stiffener nodes is connected to global unattached nodes. In addition to by using contact elements between BD and pipe the gap investigation is possible.

In this way it is also possible to investigate the effect of using contact elements, contra not.

The general BS design is illustrated in figure 34 and dimensions are for the different gap cases is given in table 9.

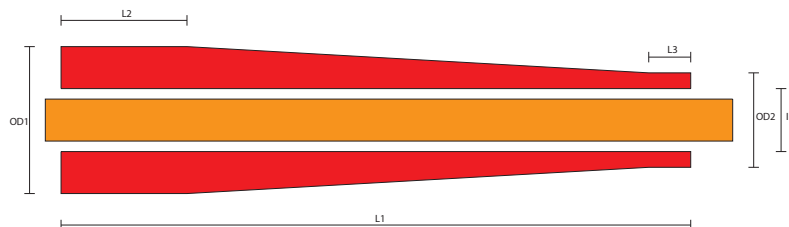


Figure 34: Bending stiffener design



Table 9: Gap cases

Case	Gap	L ₁	L ₂	L ₃	OD ₁	OD ₂	ID
1	3 mm	5000 mm	400 mm	300 mm	900 mm	500 mm	407 mm
2	6 mm	5000 mm	400 mm	300 mm	900 mm	500 mm	413 mm
3	9 mm	5000 mm	400 mm	300 mm	900 mm	500 mm	419 mm

The reduction of the bending stiffness for Case 2 and 3 compared to Case 1 is very small, and therefore this effect is neglected.

6.1.2 Lifetime data

The fatigue analysis for the local analysis is performed from the SN-approach, equation 6.1, like discussed in section 3

$$\log N = \log \bar{a} - n \log s - m \log \Delta\sigma \quad (6.1)$$

The constant m and $\log \bar{a}$ is defined from appendix B and given in table 10.

Table 10: SN-curve data

Layer	$\log \bar{a}$	n	m
Tensile armour	23.89	0	6.53
Pressure armour	12.5	0	3



6.1.3 Simulation

The simulation of the local analysis is done in two parts,

- **Part 1** Is the part where model 1 is used, there is here performed analysis for all blocks obtained from the cycle count in the global analysis. Regarding BS dimensions, CASE 2 is used.
- **Part 2** In this part model 2 is used, and there is performed a gap investigation for the three different cases. In this part, there is only performed analysis of block 1, 4 and 10 from the local analysis.

There is performed static analysis for both parts. The duration is set to be 420 seconds, where the two first seconds is used to initiate the flexible pipe elements, the 20 next is used to maintain the average value and the $\Delta\theta_{\text{cycle}}$ is performed between 20 and 400 seconds. The first part was sufficient with a incremental time step of 1 seconds to ensure numerical stability. For part 2 the needed incremental time step was set to 0.1, and due to an numerical issue regarding limit of bending stiffener strain, the stress strain curve was extrapolated to ensure numerical stability. The main simulation data is given in table 11.

Table 11: Simulation of BFLEX2010 cases

Number of Part 1 analysis	34
Number of Part 2 analysis	9
Number of steps part 1	422
Number of steps part 2	4202
Average compiling time part 1	630 seconds
Average compiling time part 2	2.3 hours

6.2 Results

6.2.1 Part 1

For the part without contact elements, the maximum stress in the inner tensile armour occur at hang off point and was smoothly distributed along down the riser,, for all time steps, like illustrated in figure 35

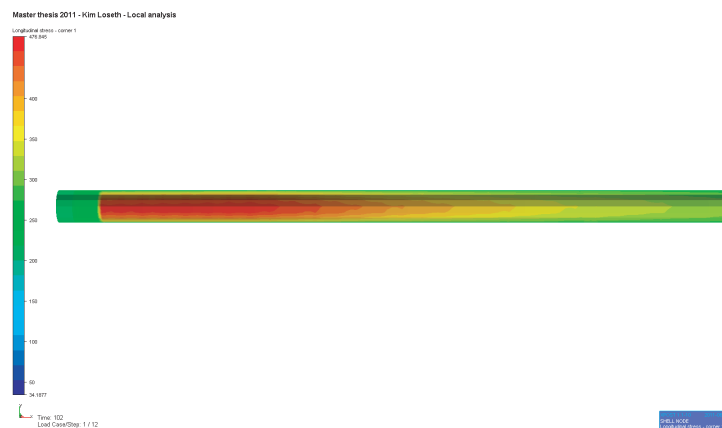


Figure 35: Maximum stress location - Block 14 - Slip regime- Part 1

And in the same way the fatigue concentration is located at the node next to hang off, figure 36.

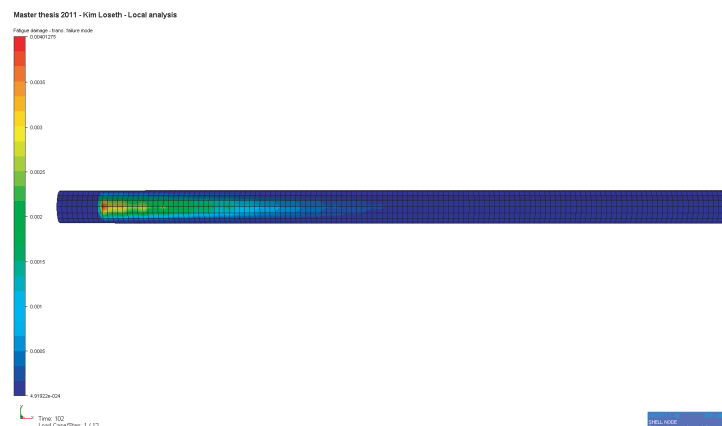


Figure 36: Fatigue distribution - Slip regime - Part 1

Not all, but a wide range of the results obtained from the part 1 analysis are given in table 12, and discussed below.



Table 12: Part 1 results

Results	Stick	Slip	Unit
Acc. Damage	3.4E-03	4.0E-3	[-]
$\sigma_{max,1}$	286.9	292.0	MPa
$\sigma_{max,4}$	337.6	341.7	MPa
$\sigma_{max,7}$	394.1	377.3	MPa
$\sigma_{max,10}$	460.5	464.7	MPa
$\sigma_{max,14}$	476.5	476.8	MPa
$\sigma_{max,17}$	479.1	-	MPa
$\sigma_{max,20}$	483.3	-	MPa
$\Delta\sigma_1$	27.5	31.4	MPa
$\Delta\sigma_4$	119.0	118.0	MPa
$\Delta\sigma_7$	232.0	217.0	MPa
$\Delta\sigma_{10}$	359.0	359.0	MPa
$\Delta\sigma_{14}$	434.0	434.0	MPa
$\Delta\sigma_{17}$	442.0	-	MPa
$\Delta\sigma_{20}$	448.0	-	MPa

The accumulate damage in table 12 are obtained from the sum of all analyzed blocks, like illustrated figure 38 for the slip regime and in figure 37 for the stick regime.

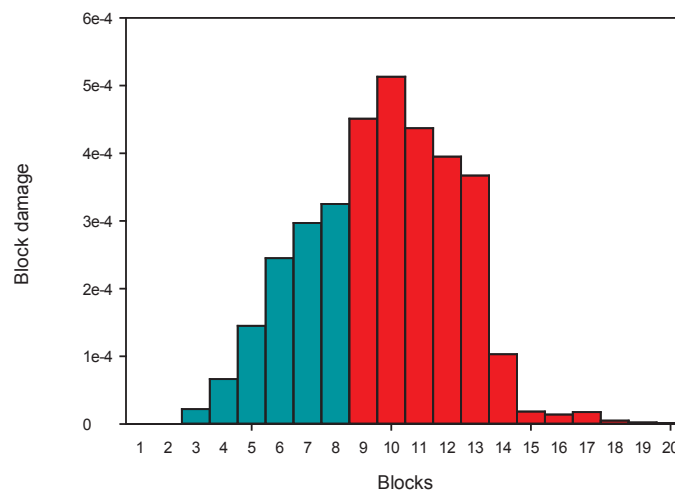


Figure 37: Block damage from stick regime

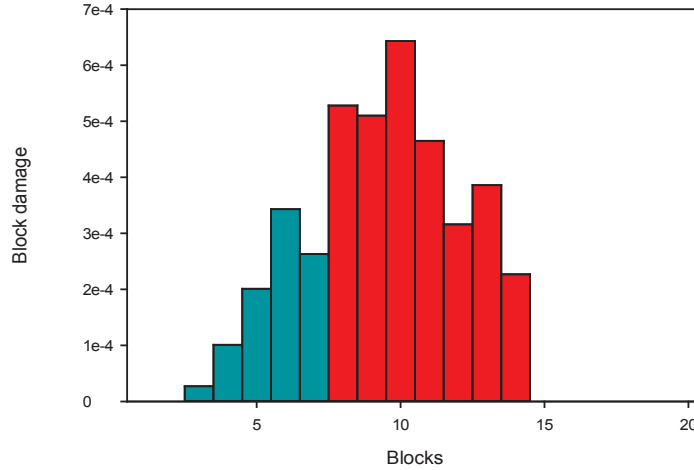


Figure 38: Block damage from slip regime

For both assumptions, the most accumulated damage are obtained from block 10. Compared to global results, the damage obtained from the largest cycle blocks are not significant. Also, due to the sudden stop in slip counting, there is not obtained any damage in block 15 to 20 and this may not be the case. Also there is an odd drop in the increasing σ_{max} trend line for block 7, this is also seen in the blocked damage diagram. The red bars represent fatigue damage caused by cases with curvature over 0.01 m^{-1} . With a accumulated damage caused by sea states representing one year, the total design life for both regime are as follows, $DFF = 10$;

$$L_{Stick} = \frac{1}{D_{Stick} DFF} = \frac{1}{3.4 \times 10^{-3} 10} = 29.4[\text{years}] \quad (6.2)$$

$$L_{Slip} = \frac{1}{D_{Slip} DFF} = \frac{1}{4.0 \times 10^{-3} 10} = 25.0[\text{years}] \quad (6.3)$$

For a normal desirable lifetime of 20 years, the calculated design lifetime (L) are on the safe side for both regimes. However there is still some uncertainty from the slip regime, due to the sudden stop of cycle counting. Regarding the stress design criteria stated in table 2 from section 1.5, the maximum tensile armour stress in normal recurrent operation should not be greater then $0.67\sigma_{Yield}$ or $0.67 \times 0.9\sigma_{UTS}$, and with a given tensile strength on 758 MPa, appendix BBBB, the criteria is 457 MPa, and not on the safe side for both regimes with a margin of 94% and 95% of the design limit.

6.2.2 Part 2

For the part 2 analysis, like part 1, the maximum stress was concentrated at hang off point under the most extreme time steps. But, opposite part 1, this is not the case for all load steps in part 2, illustrated in figure 39.

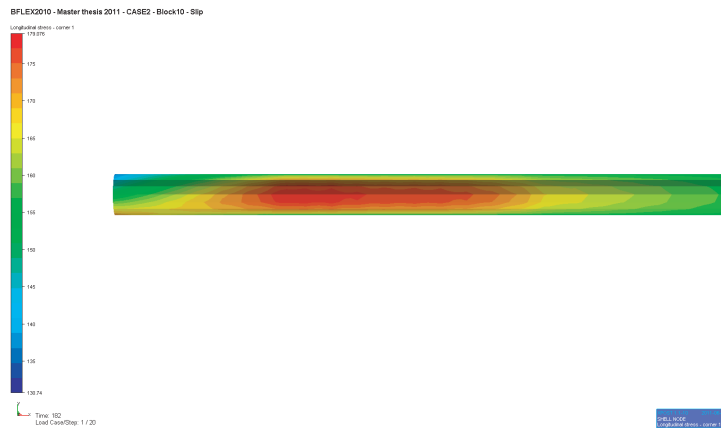


Figure 39: Stress distribution in tensile armour $t = 180$

The results of part 2 are given in table 13 and discussed below. From these results it is seen that using contact elements in the BS area, the maximum tensile stress is reduced significantly, this is also the case for the stress range $\Delta\sigma$. Regarding the gap investigation, it is seen that there are small changes in stresses during the calmest sea states, and a more significant change for large sea states, with a total increase of 7 [MPa] from case 1 to case 3 in the slip regime. To check the effect, regarding life time analysis, the damage obtained in the different cases are given in figure 40

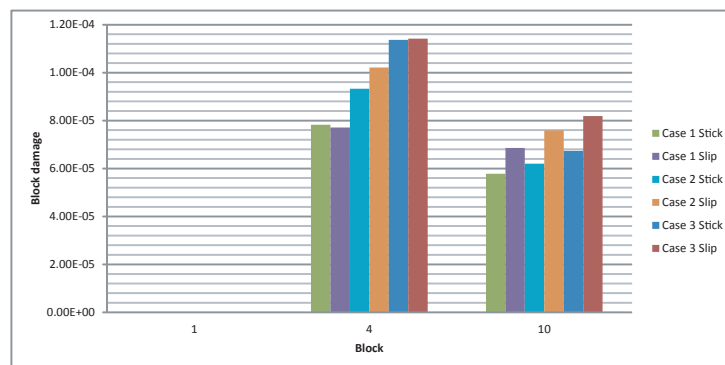


Figure 40: Fatigue damage from part 2



Table 13: Part 2 results

Case 1 results	Stick	Slip	Unit
$\sigma_{max,1}$	190.8	196.3	MPa
$\sigma_{max,4}$	259.2	266.9	MPa
$\sigma_{max,10}$	290.1	290.4	MPa
$\Delta\sigma_1$	17.7	16.0	MPa
$\Delta\sigma_4$	139.2	138.9	MPa
$\Delta\sigma_{10}$	270.1.0	269.3	MPa
Case 2 results	Stick	Slip	Unit
$\sigma_{max,1}$	191.4	197.1	MPa
$\sigma_{max,4}$	265.0	273.1	MPa
$\sigma_{max,10}$	292.2	292.8	MPa
$\Delta\sigma_1$	17.1	17.2	MPa
$\Delta\sigma_4$	143.0	145.0	MPa
$\Delta\sigma_{10}$	273.0	273.5	MPa
Case 3 results	Stick	Slip	Unit
$\sigma_{max,1}$	191.8	197.6	MPa
$\sigma_{max,4}$	268.5	276.8	MPa
$\sigma_{max,10}$	294.5	295.2	MPa
$\Delta\sigma_1$	17.1	17.5	MPa
$\Delta\sigma_4$	147.4	147.5	MPa
$\Delta\sigma_{10}$	276.5	276.5	MPa

Like part 1, there is not any significant damage caused from the first block. Also damage from block 4 is similar to damage in part 1, but when it comes to block 10 it is another story, here the damage has decreased to about 1/10 from part 1. However, this is very obvious regarding the huge drop in $\Delta\sigma$ for the 10th block. Also, it seems that the damage is more distributed along the riser with contact elements.

To investigate the effect in a more detail view the curvature distribution from the different cases is taken under consideration, for block 10 in the slip regime, it is illustrated in figure 41.

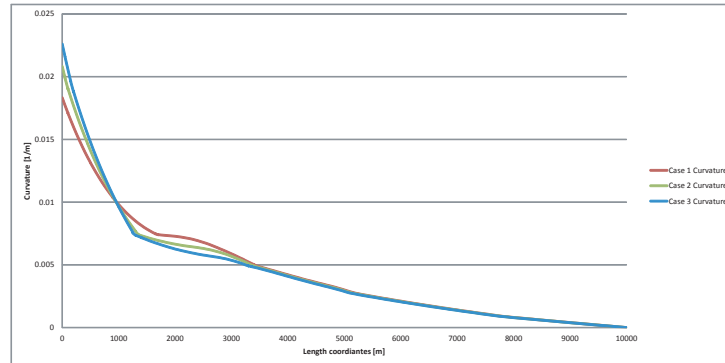


Figure 41: Curvature distribution for block 10 in slip regime, $t = 100$

In case 3, when the gap is largest, the curvature at hang off point is biggest. It seems to have a smooth curvature distribution for the first part of the BS area, until it reaches a point where it suddenly changes slope (l-coordinate, 1.25m), here it seems to create a contact with the BS and continue with a much smaller negative slope. Regarding case 1, with a smaller gap and hang off curvature, the contact seems to be achieved later into the BS area (l-coordinate, 1.5m).

In sea state 4, the effect of gap is investigated from figure 42.

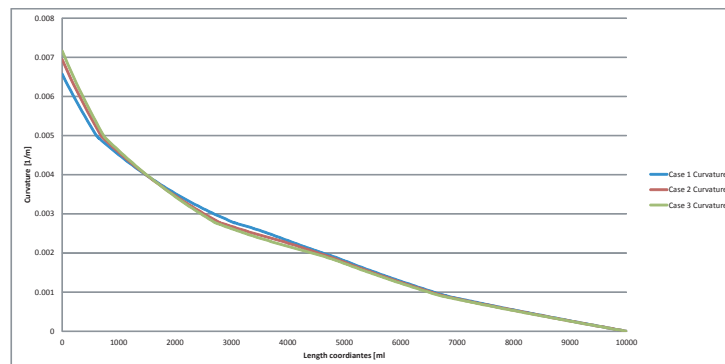


Figure 42: Curvature distribution for block 4 in slip regime, $t = 100$

Here, it seems that the effect from different gaps are small, where there are small changes for the different cases.

Regarding the design stress criteria of a flexible pipe, it is not possible to say if it satisfies the limit, since there is not performed high sea state analysis in part 2. However, by looking at the trend from the smaller blocks it seems that in this case it would be on the safe side of the criteria.



7 Conclusion

From the results in part 1 of the local analysis, it is seen that most of the fatigue damage is achieved where the pipe is in slip regime. In that way it is possible to say that the slip regime analysis performed in the global analysis represent the riser in the best way. For the different regimes there is obtained a life time period of 29.5 and 25 years, for the corresponding stick and slip regime. However, it can be assumed that the total damage would be a place between the slip and stick regime. Also, performing the local analysis, without any contact interaction with the bending stiffener caused a high amount stress in the roughest sea states, and resulting in a high amount of damage for these sea states.

From the results in part 2, where it is used contact elements between the pipe and bend stiffener, there are obtained very different results. These analysis resulted in a very large reduction of longitudinal stress in the tension armour. It also looks like that the fatigue mechanism was more distributed along the riser, compared to the very critical hot spot from part 1. However, most of the effect of using contact elements was obtained for the highest sea state, block 10, where the reduction of $\Delta\sigma$ is about 25% compared to part 1.

Regarding the gap investigation, it seems that large gaps results in larger stresses at hang off, but a more rapid decrease of stress along the riser, resulting in a better distribution of stress along the riser. The rapid decrease is a result of the contact made inside the BS, and for case 3 this is obtained closer from the hang off point compared to case 1 and 4. When looking at the gap effect for the smaller sea state, block 4, the effect of different gaps are very small. With this in mind, it could be conclude that the effect from different gaps only contribute to cases with large deflections.



8 Suggestion to further work

The further work part is divided into different blocks, like follows;

- The global analysis is performed in a very conservative way, where no direction or offset effect is included. It is therefore recommended analysis with these effects included.
- In the global analysis part, there should be performed an analysis where the whole riser, at least a part, follows the real curvature/moment relationship. Instead of performing two analysis to represent the slip/stick effect of the risers.
- Regarding the gap investigation, it could be interesting to see how far the gap could be increased before it contribute to an negative effect.
- In this thesis, only the tensile armour is looked upon. It is therefore recommended to perform in detail analysis of the pressure armour.



References

- [1] API. Ansi/api recommended practice 17b. Technical Report 4. Edition, ANSI/API, 2008.
- [2] API. Specification for unbonded flexible pipe 17j. Technical Report 3. Edition, ANSI/API, 2008.
- [3] Yong Bai and Qiang Bai. *SUBSEA PIPELINES AND RISERS*. Elsevier, London, 1st, edition, 2005.
- [4] S. Berge, A. Engseth, I. Fylling, C.M. Larsen, B.J. Leira, and A. Olufsen. Handbook on design and operation of flexible pipes. *FPS2000*, 1992.
- [5] Stig Berge. Fatigue design of welded structures. Technical report, Department of Marine Technology, NTNU, 2006.
- [6] Mikael Braestrup, Jan Bohl Andersen, Lars Wahl Andersen, Mads Bryndum, Curt John Christensen, and Niels-Jørgen Nilsen. *Design and Installation of Marine Pipelines*. Blackwell Science, Oxford, 1st, edition, 2005.
- [7] Kenneth Eik and Einar Nygaard. Statfjord late life metocean design basis, 2003.
- [8] O.M. Faltinsen. *Sea loads on ships and offshore structures*. Cambridge ocean technology series. Cambridge University Press, 1993.
- [9] F. Grealish, R. Smith, and J. Zimmerman. New industry guidelines for fatigue analysis of unbonded flexible risers. *OTC 18303*, 2006.
- [10] Steinar Kristoffersen. Statoil’s operational experience with flexible risers. In *Offshore Pipe Lines And Risers*, 2010.
- [11] Ivar Langen and Ragnar Sigbjørnsen. *Dynamisk analyse av konstruksjoner*. Tapir, 1986.
- [12] Nils Sødahl, Geir Skeie, Oddrun Steinkjer, and Arve Johan Kalleklev. Efficient fatigue analysis of helix elements in umbilicals and flexible risers. *OMAE2010-21012*, 2010.
- [13] Svein Sævik. SIMLA- theory manual. *MARINTEK*, 2008.
- [14] Svein Sævik. BFLEX2010- theory manual. *MARINTEK*, 2010.



- [15] Svein Sævik. BFLEX2010- user manual. *MARINTEK*, 2010.
- [16] Svein Sævik, Ole David Økland, Gro Sagli Baarholm, and Janne K.Ø. Gjøsteen. SIMLA version 3.15.0 user manual. *MARINTEK*, 2010.
- [17] Det Norske Veritas. DNV-RP-C203 Fatigue Design of Offshore Steel Structures. Technical report, DNV, 2010.
- [18] Y. Zhang, B. Chen, L. Qui, T. Hill, and M. Case. State of the art analytical tools improve optimization of unbonded flexible pipes for deepwater environments. Technical Report 15169, OTC, 2003.



A Flexible riser data

1. DESCRIPTION OF PIPE DATA

1.1 Pipe data sheet

The pipe data sheet is presented below:

Inside diameter	228.6 mm	Service	Sour dynamic	Max Fluid Temp	130.0 °C	
Design pressure	50.07 MPa	Conveyed Fluid	Oil	Water Depth (m)	300.0 m	
Layer	Material	Strength (MPa)	I.D. (mm)	Thick (mm)	O.D. (mm)	Weight (kg/m)
Carcass	Steel	689	228.60	7.00	242.60	23.786
Antiwear	PVDF		242.60	3.99	248.60	4.097
Barrier	PVDF		248.60	12.00	272.60	17.389
Antiwear	PVDFc		272.60	1.02	274.63	0.873
Z-spiral	Carbon Steel	758	274.63	12.00	298.63	68.762
Flat spiral	Carbon Steel	758	298.63	5.99	310.62	40.835
Antiwear	PA11 (nylon)		310.62	1.52	313.67	1.569
Tensile_armour_ 1	Carbon Steel	758	313.67	5.99	325.66	43.049
Antiwear	PA11(nylon)		325.66	0.41	326.47	0.425
Antiwear	PA11(nylon)		326.47	1.52	329.52	1.649
Tensile_armour_ 2	Carbon Steel	758	329.52	5.99	341.51	45.400
Antiwear	PA11(nylon)		341.51	0.41	342.32	0.445
Antiwear	PA11(nylon)		342.32	1.52	345.37	1.729
Tensile_armour_ 3	Carbon Steel	758	345.37	5.99	357.36	46.991
Antiwear	PA11(nylon)		357.36	0.41	358.17	0.466
Antiwear	PA11(nylon)		358.17	1.52	361.22	1.808
Tensile_armour_ 4	Carbon Steel	758	361.22	5.99	373.21	49.265
Antiwear	PA11(nylon)		373.21	0.41	374.02	0.487
Antiwear	PA11(nylon)		374.02	0.41	374.83	0.319
Protective sheath	PA11(nylon)		374.83	12.00	398.83	15.312

Table 3.1 Pipe Data Sheet

The steel tendon cross-section details are summarised below. Details on the geometry is provided by separate text input file in Bflex format for the Z-spiral.

Layer	Dimension (mm)	Pitch (mm)	Wires	Angle (°)	Filled (%)
Carcass	55 × 1.4	-	-	-	-
Z-spiral	26.8 × 12	-	-	-	-
Flar spiral	16 × 6	-	1	-	-
Tensile_armour_1	12 × 6	1039.9	54	44	91.3
Tensile_armour_2	12 × 6	1091.5	57	44	91.8
Tensile_armour_3	12 × 6	1225.9	61	42	90.7
Tensile_armour_4	12 × 6	1281.2	64	42	91.0

Densities to be based on data sheet values using the combined weight and thickness values provided. The overall pipe mass in empty condition is 364.65 kg/m. During operation (oil filled condition – oil density = 800 kg/m³) the mass increases to 399.1 kg/m³. In the laboratory test condition, the mass will be 407.7 kg/m³. The buoyancy mass to be calculated based on the external diameter and a sea water density of 1025 kg/m³.

Note that the layer weights in combination with the density and cross-section area given can be used to calculate the lay angle of the helices by the simple formula:

$$\alpha = \cos^{-1} \left(\frac{\rho_{layer} A}{m_{layer}} \right)$$

The geometry of the carcass can be handled according to an example input provided and the basic principles outlined in below figure utilizing the layer thickness and the thin plate (dimension 1.4*55 mm) used to form the carcass.



Mechanical properties are given below.

Material	Young's modulus (MPa)	Poisson's ratio (-)
Steel	2e5	0.3
Plastic layers	300	0.4

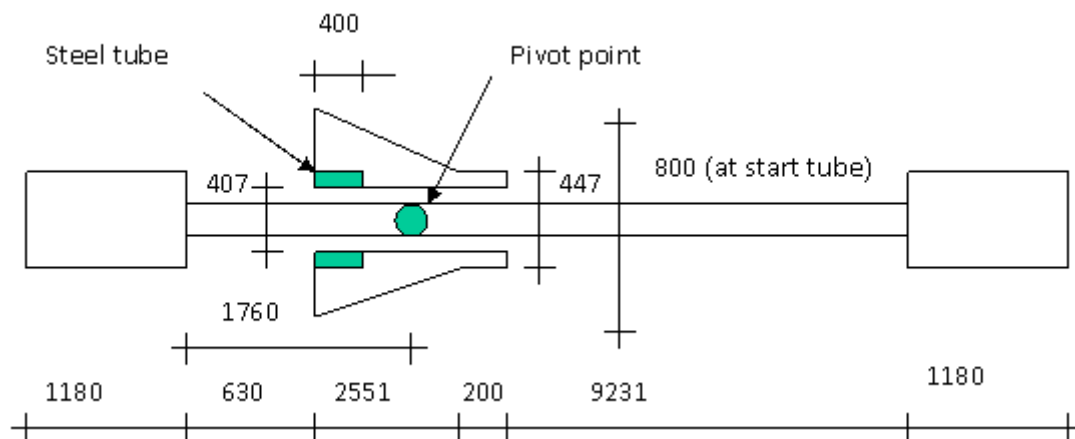
1.2 Description of bend stiffener

The pipe bending stiffener is normally made of polyurethane (PU). The Young's modulus of elasticity during operation is taken to be 68.5 MPa. During testing at room temperature ((23 °C), the stress strain curve given below governs

Strain (%)	Stress (MPa)
1	2
2	4
3	5.2
4	6.4
5	7.2
6	8
7	8.6
8	9.2
9	9.7
10	10.2

It is seen that the tangential modulus of elasticity is 200 MPa up to 2% strain.

The geometry of the pipe and bending stiffener to be used for test specimen modelling in Bflex is shown in Figure 3.1 below. The figure also includes the position of the specimen relative to the test rig pivot point in the laboratory test rig (for the riser model project only the bend stiffener geometry is relevant).



1.3 Fatigue data

With regard to the fatigue calculation, example input files are provided on Bflex format. The fatigue data to be used are specified below:

$$\lg N = \lg a - n \lg s - m \lg \Delta \sigma$$

where $\lg a$ is a constant, $\lg s$ is the standard deviation, n is the number of standard deviations used to construct the fatigue curve and m is the slope parameter where:

Layer	$\lg a$	n	m
Tensile_armour_	23.89	0	6.53
Z-spiral	12.5	0	3

1.4 Operational data

Internal pressure to be applied is 475 bar (47.5 MPa).

1.5 Load cases to be applied for the test rig case (not relevant for the full riser analysis)

For the test rig case, the following load sequence is to be assumed:

LC1 – 400 000 cycles at variable rocking angle +/- 7.5 degrees and constant tension 725 kN

LC2 – 200 000 cycles at variable rocking angle +/- 12.5 degrees and constant tension 750 kN

1.6 Friction coefficients

Between steel and plastic – 0.15

Between steel and steel (for Z-spiral) – 0.25



B Cross Sectional Properties

Table I Power cable and riser departure position and angles

Name	x (m)	y (m)	z (m)	Top angle (degree)	Azimuth angle (degree)
OPR	51.0	-1.15	21.5	9.5	5.24

Table II Sectional properties of the oil production riser (bending stiffener part not included)

Segment	Line length, from to [m]	Marine growth [mm]	Property	Unit	Value
A	11	0	Mass	kg/m	399
			Outer diameter	m	0.399
			Transverse drag coefficient	[-]	1.05
			Tangential drag coefficient	[-]	0.01
B	41	60	Mass	kg/m	510
			Outer diameter	m	0.519
			Transverse drag coefficient	[-]	1.05
			Tangential drag coefficient	[-]	0.01
C	330	30	Mass	kg/m	451
			Outer diameter	m	0.459
			Transverse drag coefficient	[-]	1.05
			Tangential drag coefficient	[-]	0.01
D	150 Buoyancy section	30	Mass	kg/m	399
			Outer diameter	m	
			Transverse drag coefficient	[-]	0.76
			Tangential drag coefficient	[-]	0.20
E	25	30	Mass	kg/m	451
			Outer diameter	m	0.451
			Transverse drag coefficient	[-]	1.05
			Tangential drag coefficient	[-]	0.01